Mapping of the intertidal shores of Parque Natural do Litoral Norte

Hugo Sainz Meyer
Mestrado em Deteção Remota
Departamento de Geociências, Ambiente e Ordenamento do Território 2021

Orientador
Doutora Cândida Maria Gomes Vale, Investigadora do CIIMAR

Coorientador
Professor Doutor José Alberto Álvares Pereira Gonçalves, Professor, Faculdade de Ciências da Universidade de Porto

U.PORTO

FACULDADE DE CIÊNCIAS
UNIVERSIDADE DO PORTO

Todas as correções determinadas pelo júri, e só essas, foram efetuadas.

O Presidente do Júri,

Porto, ______/______/_________

MSc

Agradecimentos

Primeiro gostaria de agradecer à minha orientadora, Doutora Cândida Vale, investigadora do CIIMAR, Centro Interdisciplinar de Investigação Marinha e Ambiental, tenho a certeza que este trabalho não teria sido feito sem a sua imensa ajuda, dedicação e mão dura. Gostaria também de agradecer ao meu coorientador, Professor Doutor José Alberto Gonçalves, pela sua ajuda e orientação.

Agradeço muito aos meus colegas Óscar Babé Gómez e Silvia Chemello por estarem sempre prontos para ajudar no que fosse. Não posso esquecer a Marta Martins, que me ajudou e motivou durante este longo percurso. Quero ainda agradecer ao Rui Seabra por toda a sua ajuda e disponibilidade durante todo este processo. Por último queria agradecer a Francisco Arenas por ser o mentor de este trabalho e quem me meteu em toda esta confusão do qual estou muito agradecido.

Resumo

A deteção remota é uma ferramenta muito poderosa para a criação de mapas topográficos da superfície terrestre. Dados de satélite, fotografias aéreas e mais recentemente os veículos aéreos não tripulados (drones) têm sido utilizados para este propósito. Comparada com os outros métodos, os dados obtidos com os *drones* têm uma resolução superior. Os *drones* apresentam numerosas vantagens, especialmente em trabalhos em áreas intertidais onde as condições são mais duras (e.g. ventos, chuva). O Parque Natural do Litoral Norte é uma área protegida onde coexistem vários ecossistemas com uma grande biodiversidade, maioritariamente em zonas intertidais rochosas. Para os organismos que habitam estas áreas, a temperatura é um dos fatores mais importantes na sua sobrevivência. Nesta tese foi testado o potencial dos *drones* para produzir mapas topográficos de elevada resolução no intertidal de quatro praias do Parque Natural do Litoral Norte. Para o efeito, utilizaram-se dois *drones* diferentes (Phantom 4 Pro e FIMI SE X8) na captação de imagens usadas posteriormente para a construção dos mapas topográficos (modelos digitais de elevação) dos quatro intertidais. A partir destes foram derivadas as variáveis topográficas mais importantes (Orientação, Pendente e Radiação Solar). A temperatura foi obtida a partir de *loggers* previamente colocados em locais estratégicos destes intertidais rochosos. Esta demonstrou-se correlacionada com as variáveis topográficas mais relevantes (Orientação, Pendente e Radiação Solar), para que fossem construídos dois modelos de temperatura superficial da rocha. Por fim, os modelos de temperatura da superfície da rocha foram projetados para a totalidade da área rochosa das quatro praias. Dois modelos extremos de temperatura da superfície da rocha foram criados – mínimo (R^2= 0,87) e máximo (R^2=0,75) – que ilustram grande variabilidade nas áreas de estudo. Esta tese demonstra o desafio que é fazer mapas topográficos em áreas como a zona intertidal. Para além disso, enfatiza a importância da criação de modelos de temperatura da superfície da rocha que podem ser usadas para estudar o impacto das alterações climáticas em organismos sésseis. Esta tese revela novas ferramentas de grande potencial para serem desenvolvidas e utilizadas para estudar, proteger e conservar estes ecossistemas.

Abstract

Remote sensing is a powerful tool for the creation of topographic maps of the earth's surface. Satellite data, aerial photography and, more recently, unnamed aerial vehicles (UAVs) have been used for this purpose. Among these, drones provide data with better spatial resolution and present numerous advantages, especially when working in intertidal areas which bear rough conditions (e.g. winds, rain). The Parque Natural do Litoral Norte (PNLN) is a protected area which encompasses several ecosystems of great biodiversity, particularly in intertidal rocky areas. Temperature is the most important factor for the survival of intertidal organisms. In this thesis the potential of drones to produce high resolution topographic maps was assessed in four intertidal areas of PNLN. Two different drones (Phantom 4 Pro and FIMI SE X8) were used to create a topographic map (Digital Elevation Model) of the four study areas, from which the important topographic variables (Aspect, Slope, Solar Radiation) were derived. Data on local temperature were obtained from loggers, previously placed in strategic locations of rocky shores. They were related with relevant topographic variables, to build two models of rock surface temperature. Finally, the rock surface temperature models were projected to the entire surface area of the four intertidal areas. Two extreme rock surface temperature models of the four rocky shores were created - minimum and maximum – minimum (R^2= 0,87) and maximum (R^2=0,75) – which illustrate high variability in the study areas.

This thesis shows how challenging it is to create topographic maps of areas such as the intertidal. Furthermore, it highlights the importance of the creation of rock surface temperature models which can then be used to study the direct effect of temperature changes on sessile species. This uncovers new tools with great potential to be further developed and be used to study, protect and conserve these environments.

Key words: Remote sensing, UAVs, Drones, Digital elevation model, Temperature, Rocky shores, Surface Temperature Model.

Index

Index of Figures

Index of Tables

Acronyms

DEM – Digital Elevation Model

ESRI – Environmental Systems Research Institute

ETRS – European Terrestrial Reference System

GNSS – Global Navigation Satellite System

GCP – Ground Control Point

HMSL – Height above Mean Sea Level

ICNF – Instituto da Conservação da Natureza e das Florestas

PNLN – Parque Natural do Litoral Norte

RTK – Real Time Kinematic

ReNEP – Rede Nacional de Estações Permanentes

RS – Remote Sensing

UTM – Universal Transverse Mercator

UAV – Unmanned Aerial Vehicles

1. Introduction

Remote sensing (RS) is a powerful tool for the creation of topographic maps of the earth's surface. It is the science of acquiring information about an object, area or phenomenon through analysis of the energy reflected by the earth's surface sensed by a device (sensor) which is not in direct contact with the target object (Chuvieco, 2020). Although dominated by the use of satellite data, which provide the ability of mapping large areas at the same time (Kwok, 2018), the emergence of unmanned aerial vehicles (UAVs) has created new opportunities for RS application in several research (Pádua et al., 2017, 2018). UAVs are aircrafts which have no pilot on board. Usually called *drones*, these devices are remotely controlled from the ground by an operator or can be pre-programmed to work in autopilot mode (Marx et al., 2017). The UAVs have an original military purpose, being only applied to research studies in the late 90s and early 21st century (Colomina & Molina, 2014). In the last decade, an immeasurable number of UAV manufacturers have emerged due to technological advances and more permissive legislation (Pádua et al., 2017). UAVs have the unique ability to capture data at a spatial, spectral and temporal resolution never seen before (Maes & Steppe, 2019). The wide variety of sensors that UAVs currently have (e.g. thermal cameras and hyperspectral cameras), means that the data they acquire can generate a huge range of products, such as digital elevation models (DEM), orthophotomaps and vegetation indices, which are widely used in different fields (Mozaffari et al., 2019). Therefore, they have been used in many studies in countless research fields, such as like ecology, agriculture and disaster protection (Yao et al., 2019).

Ecology is one of the research areas which had greatly benefited from remote sensing data to study natural processes at global scale. The North American Breeding Bird Survey (BBS, https://www.pwrc.usgs.gov/bbs), United States Forest Inventory and Analysis National Program (FIA, http://www.fia.fs.fed.us) are examples of monitoring projects using satellite data (long time series data) at a global scale (Zhang et al., 2016). In this context, the appearance of UAVs has revolutionized this field of knowledge. UAVs surveys have low flight altitude and therefore, the resulting data have very-high spatial resolution (pixel sizes in the order of centimeters; Mancini et al., 2013). By detecting changes at very small scales, UAVs enable the study of ecological processes with a very high resolution (Cruzan et al., 2016; Puliti et al., 2015; Vincent Raoult et al., 2020). Also, data might be acquired across relatively large areas with great flexibility in the timing and frequency of image capture, which allows spatial and temporal dynamics to be added (Anderson & Gaston, 2013). The first studies made with the help of drones in terrestrial ecology were to monitor population size of black-headed gull (Jones et al. 2006). Baena et al. (2017) and

Johansen et al. (2020) have studied the health condition of trees through the state of its leaves by measuring their absorbance capacity with UAV flights. These equipments have brought a new way for ecologists to study and understand natural processes over small to medium sized regions (Vincent Raoult et al., 2018). They offer an unprecedented opportunity to study and monitor coastal environments.

1.1 Coastal ecosystems

Coastal areas are regions of remarkable primary and secondary productivity, biodiversity, and high accessibility, which support numerous physical and biological processes. Considering the rough conditions of these areas (e.g. tides, winds, waves and currents), the use of UAVs brought numerous advances, as it made studies less time consuming and resource-intensive (Colefax et al., 2018; Schofield et al., 2019). Indeed, this new approach have prompted ecological studies in coastal areas (Murfitt et al., n.d.; Rossiter et al., 2020), helping their ecological management (Kiszka et al., 2016; Raoult & Gaston, 2018). Among them are the mapping of seaweeds communities conducted in Portugal (Borges et al., 2019).

In coastal areas, the intertidal zone is defined as the boundary between the terrestrial and marine environments (Lv et al., 2020). Intertidal zones create diverse ecosystems with unique conditions influenced by the ocean and the land (Nordlund et al., 2013). Within these areas, the rocky intertidal zones are places affected by winds, wave energy, tides and many other physical factors (Hawkins et al., 2019; O'Donnell & Denny, 2008). Despite the physical conditions, these are places with high biodiversity, particularly in a small space. Their physical and ecological characteristics make them ideal places to apply remote sensing technologies, such as UAVs (Borges et al., 2019; Escobar-Sánchez et al., 2021). The work carried out with UAVs offers a new methodology that is much less destructive for the organisms that live there.

The intertidal and rocky shore organisms are highly adaptable to fast and extreme changes (Faria et al., 2020). Despite all the physical parameters affecting them, temperature plays a crucial role on their survival capacity (Li et al., 2021; Wang et al., 2020). All the residents of these areas have to struggle twice a day to survive with the temperature of the rock where they live (Judge et al., 2018; Schneider et al., 2010; Sinclair et al., 2016). When the weather conditions are extreme, the surface of the rock in these areas can become lethal due to the increase or decrease of the temperature (Seabra et al., 2011). With the help of UAVs, it has been possible to derive surface temperature models with a very high level of detail (Garza, 2016). Intertidal ecology can benefit from these models associated to physical data taken in situ, with the help of loggers (Fitzhenry et al., 2004; Lima & Wethey, 2009; Miner et al., 2018). Together they create rock surface temperature models that help to understand and conserve the different habitats that exist in these places (Choi et al., 2019). Therefore, it is important to characterize the temperature surface of each intertidal to further understand the ecology of the organisms that inhabit these places, how they are distributed and how they will be affected by the coming climate changes.

The Parque Natural do Litoral Norte (PNLN) presents one of the largest rocky intertidal concentrations in Portugal (ICNF, 2018) (Fig. 1). These places are home to many commercially important and heavily exploited species, namely *Paracentrotus lividus*, that need to be studied and conserved (Bertocci et al., 2021). Being a protected area, regulations on the catch of intertidal organisms are in place, for instance, it is not allowed the use of tools for the collection of organism and width and size of organisms harvested are also limited (Bertocci et al., 2021; ICNF, 2018). Other activities such as artisanal fisheries, *Sargaço* collection and an original agricultural method, *masseiras* (plantations are close to dunes and use *Sargaço* and *Polybius henslowii* crabs as fertilizer) are traditional of this location and are still preserved nowadays (ICNF, 2018). Given that these are already exploited and damaged locations and bearing in mind that this is a protected area, research with drones are ideal, as they present the possibility of studying these locations with a minimum damage while enabling protection.

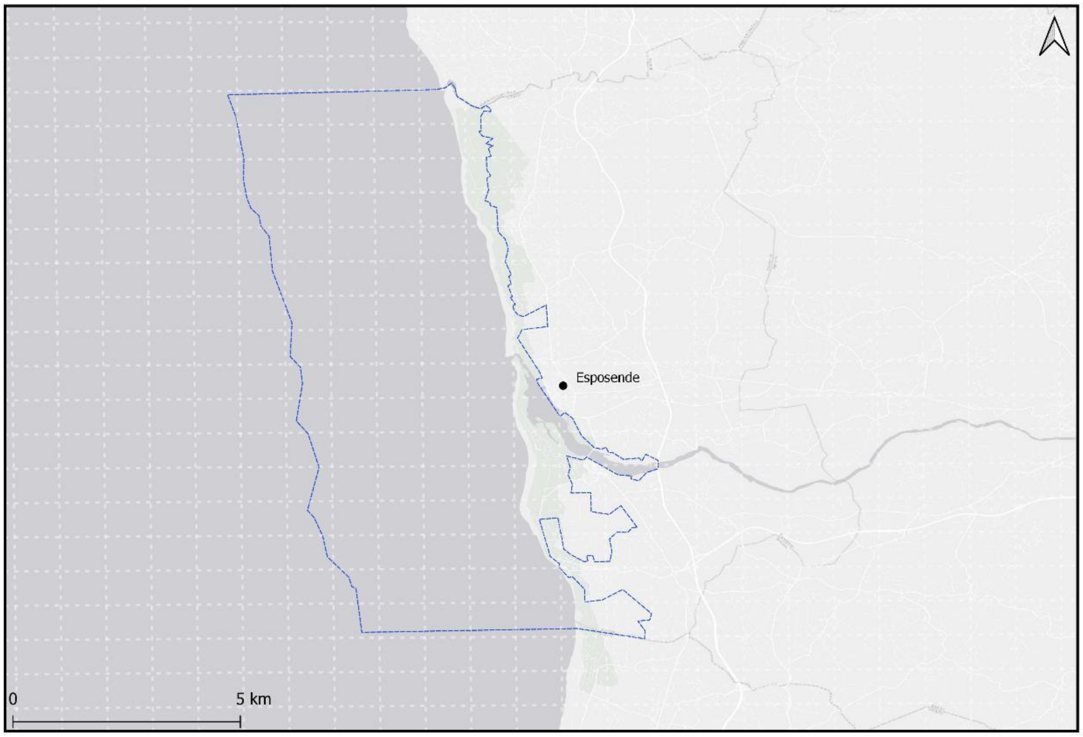

Figure 1: Geographical representation of the limits of Parque Natural Litoral Norte, in the northern coast of Portugal.

1.2 Objectives

Coastal ecosystems are highly dynamic environments and therefore very susceptible to multiple threats, including climate change. Mapping and monitoring are essential to better understand and manage these ecosystems. The main aim of this thesis was to map, with the highest possible resolution, the intertidal rocky shore of four rocky shores of Parque Natural do Litoral Norte. This aim was branched in two specific objectives: the first was to make topographic spatial characterization of the rocky intertidal areas of the four study areas. The second one was to build a temperature surface model for these rocky shores. To build this model, data collected with UAVs were combined with temperature data collected from loggers placed in the intertidal rocks. Due to the inherent challenges of working in coastal areas, biophysical datasets at appropriate spatial and temporal scales are seldom available. This thesis will be a step forward in the development of a rocky shore surface model that will be a useful tool for a better understanding of ecological processes on a local scale.

1.3 Thesis structure

This thesis is organized in four chapters. The first chapter is the Introduction with the brief revision of the topics addressed in the following chapters, as well as the objectives of this work. The second chapter describes the techniques, methodological and statistical approach used to analyse the data collected. The third chapter presents the results obtained from each of the processes conducted in each of the phases of this work. Finally, chapter 4 contains the discussion and conclusions as well as future perspectives.

2. Methodology

2.1 Study Area

The study area is in northern west coast of Portugal and encompasses four rocky intertidal shores, Carrugem, São Bartolomeu do Mar, Rio de Moinhos and Apúlia (from north to south – Figure 2). These rocky shores are embraced by Parque Natural do Litoral Norte (PNLN). The PNLN extends over 16 km of coastal Atlantic, with a total size of 88,87 km^2, out of which the vast majority is marine protected area (~76,53 km^2) and the remaining is land area (ICNF, 2018). The former is essentially made up of a sandy beach cordon and primary and secondary dunes of great instability and at risk of erosion. The climate in the park is strongly influenced by the Atlantic Ocean, with abundant rainfall during the winter and constant northern winds. The target rocky shores are formed by granite rocks, schistose and conglomerates and are surrounded by coarse sands, boulders and smalls rocks (*Geologia | Hidrologia | Clima — ICNF*, n.d.).

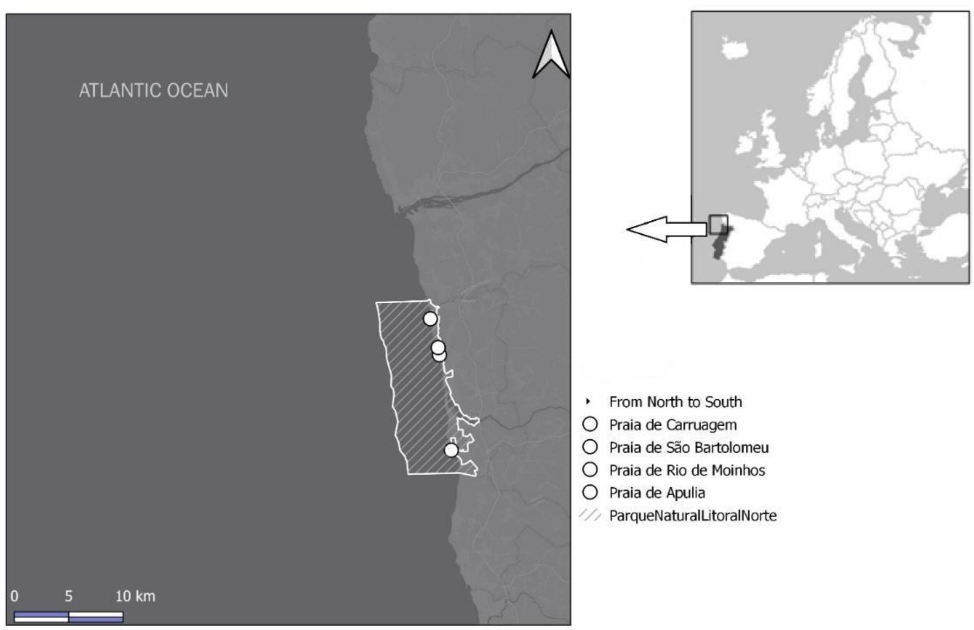

Figure 2: Location of the northern west of continental Portugal and the study intertidal shores: Carruagem, São Bartolomeu de Mar, Rio de Moinhos and Apúlia.

The intertidal zone is the interface between land and ocean. Intertidal shores may be divided into three different levels: High, Medium, Low. This division is based on the tidal level that reaches different heights of the shore (Widdows & Brinsley, 2002).

The High intertidal zone is an area that is only covered by sea water during high tides, and for a short period of time. As it is dry for long periods, this area is inhabited by small marine snails, barnacles, hermit crabs and by a group of algae (e.g. *Fucus vesiculosus)* that can withstand these tough conditions (Nicastro et al., 2013). The Middle intertidal zone is the place where the tide rises and falls twice a day. A larger number of organisms can be found in this area, such as sea urchin, crabs, mussels, biogenic reefs and different types of algae *(*e.g. *Mytilus* spp*)* (Raffaelli & Hawkins, 1996). The Low intertidal zone is always covered by water, except during spring low tides, this area constitute a protection and growth zone for many species, so a large number of organisms can be found (*NOAA's National Ocean Service*, n.d.).

In the four rocky shores, the high intertidal is dominated by green and brown seaweeds, consisting mainly of *Enteromorpha spp* and *Fucus vesiculosus*. The middle zone is constituted by large patches of *Mytilus* spp, barnacles and limpets. In the low intertidal zone it is possible to find some biogenic reefs, formed by the polychaete *Sabellaria alveolata*, and big areas dominated by red algae including *Chondrus crispus*, *Osmundea pinnatifida* and some opportunistic kelp like *Saccorhiza polyschides* and *Laminaria ochroleuca.*

2.2 Intertidal zone mapping / Physical data collection

UAV flights were conducted between January 2020 and February 2021. The weather conditions were challenging, with flights being always done in low tide conditions and early in the morning, so that there would be low wind and minimal cloud cover. The first and second campaigns were conducted with the Xiaomi FIMI X8 SE UAV on the intertidal areas of São Bartolomeu and Apúlia. Flights with the DJI Phantom 4-Pro UAVs, were carried out at the end of 2020 and the beginning of 2021 in Moinhos and Carruagem (Table 1). In one of the campaigns, one of the drones was damaged by the wind, reason for which there was a need to use two different drones characteristics of both models of drones are described in Table 2.

Table 1: Dates of the campaigns and drones used for each study area.

STUDY AREA	DATE	UAV
Carruagem	21 NOVEMBER 2020 09:08	DJI PHANTOM 4-PRO
São Bartolomeu	14 FEBRUARY 2020 10:33	XIAOMI FIMI X8 SE
Moinhos	26 FEBRUARY 2021 08:31	DJI PHANTOM 4-PRO
Apúlia	24 JANUARY 2020 09:33	XIAOMI FIMI X8 SE

All flights were performed in parallel rows with high longitudinal and lateral overlap. They were programmed using the software *Pix4Dcapture* in which the target area, the longitudinal and lateral overlap, the ground pixel size and the flight direction were previously planned. A dual-frequency GNSS receiver (Trimble R6-3) in real-time kinematic (RTK) mode, with real-time differential correction broadcast by the National Network of Permanent Stations (ReNEP), was used to collect the ground control points (GCPs). This was performed to improve the georeferencing of the images collected, because the global navigation satellite system (GNSS) included in UAVs has an accuracy with an associated error of a few meters. To improve the geolocation accuracy of the products extracted from the photographs, it is necessary to capture a series of GCPs uniformly over the study area (Table 3 and Fig. 3).

Table 2: Characteristics of the drones.

	X8SE	PHANTOM 4 PRO
MANUFACTURER	Xiaomi Fimi	DJI
WEIGHT	765 grams	1388 grams
MAX FLIGHT TIME	35 minutes	30 minutes
DRONE MAX SPEED	65 km/h	72 km/h
CAMERA SENSOR	SONY CMOS	CMOS
DRONE IMAGE STABILIZATION	3 axis gimbal	3 axis gimbal
DRONE PHOTO RESOLUTION	12 Mp	20 Mp
SATELLITE POSITIONING SYSTEMS	GPS GLONASS BEIDOU	GPS GLONASS
IMAGE FORMAT	DNG, PNG	JPEG, DNG

Table 3: Example of some GPCs captured in one of the intertidal, HMSL represents the orthometric altitude coefficient for each of the points.

POINT	LONGITUDE (Decimal degrees)	LATITUDE (Decimal degrees)	HMSL (m)
P01	-8.806199472	41.597441824	4.831
P02	-8.806232568	41.596617771	4.449
P03	-8.806095169	41.595723667	3.887

Loggers were installed in three intertidal zones (Carruagem, Moinhos and Apúlia). Due to technology/equipment constrains, a different number of loggers was placed in each intertidal zone, namely four in Carrugem and Apúlia and six in Moinhos (Fig. 4). Each of these loggers was positioned with different orientation with the objective of capturing temperatures at which intertidal organisms are exposed during the low tide (Judge et al., 2018; Seabra et al., 2011). They were installed by drilling small holes in the rock surface and coated with epoxy. Loggers were programmed to record the temperature of the rocky surface each ten minutes. Data matching the dates of the drone flights were collected from the loggers (Gandra et al., 2015).

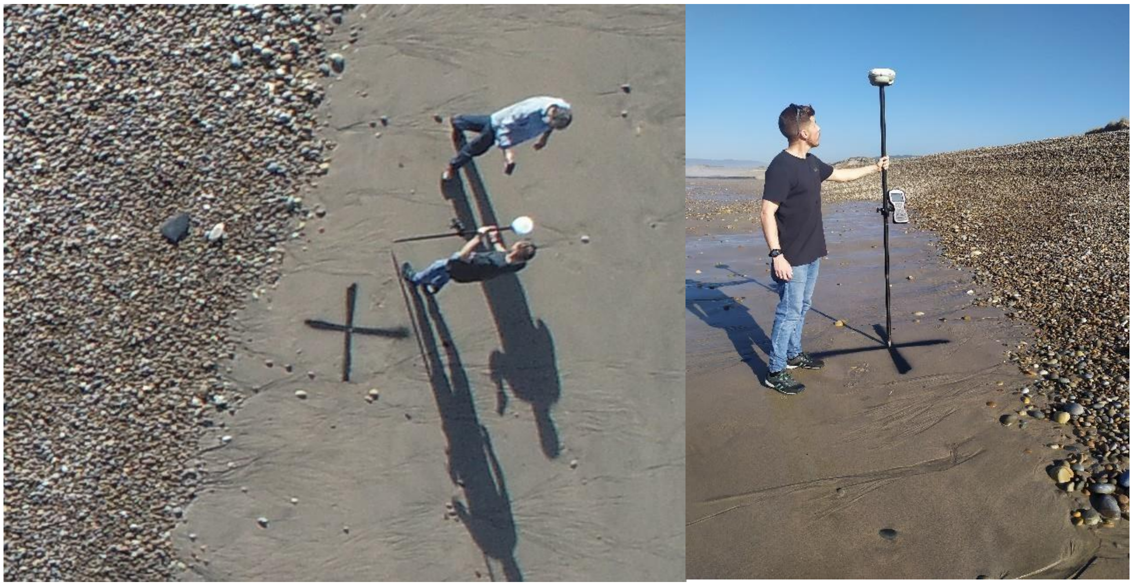

Figure 3: Representation of the process to collect GCPs.

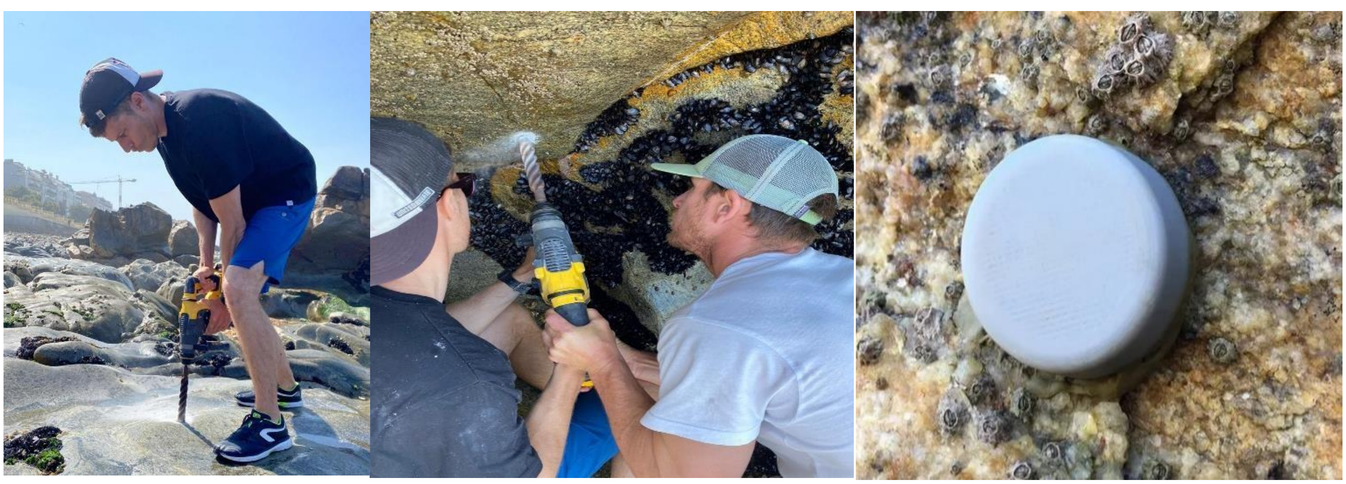

Figure 4: Set up of loggers in the rocky intertidal.

2.3 Data processing

The alignment of the images captured with UAVs and their georeferencing was processed using photogrammetric methods implemented in the software Agisoft Photoscan (Agisoft LLC, St.

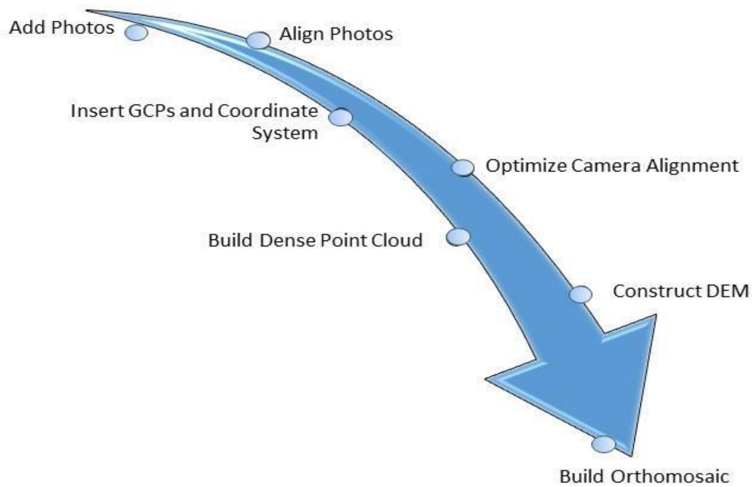

Figure 5: Schematic workflow in Agisoft PhotoScan software.

Petersburg, Russia). The coordinate system in which the images were captured by the UAVs was reprojected for the ETRS89 UTM Zone 29N reference system. It was then aligned with the highest possible resolution, creating a 3D sparse point cloud generated from conjugate points and, afterwards, the GPCs were added (Fig. 5). A dense cloud point was obtained with a surface model in a grid. Finally, using the dense cloud point, orthorectification was performed to generate the digital elevation model (DEM) for each of the intertidal rocky areas (Fig. 6) (Gonçalves et al., 2018).

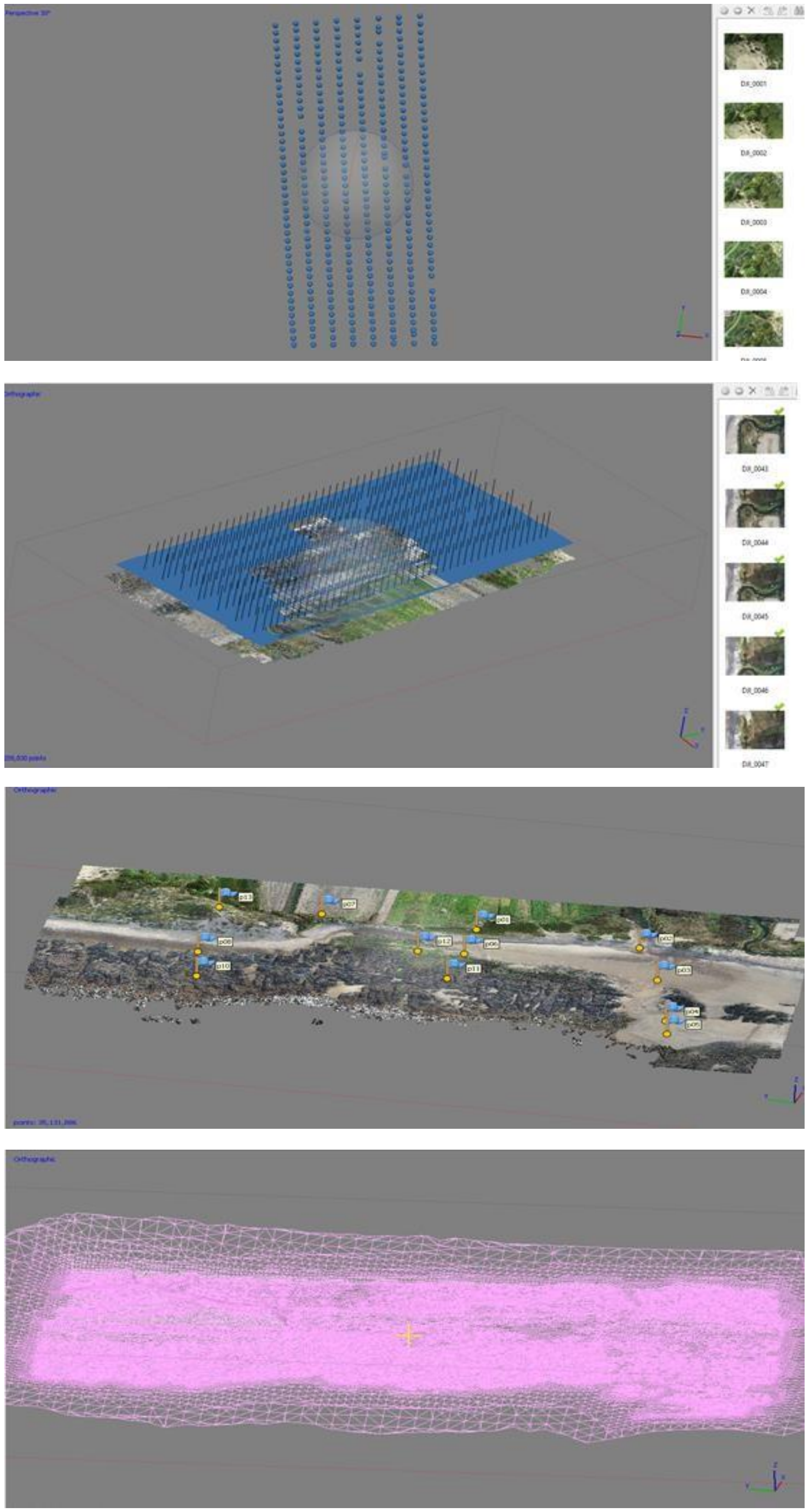

Figure 6: Workflow in a Agisoft Photoscan software. Top left: addition of the photographs taken during the flight. Top right: alignment of the photographs. Bottom left: addition of the GCPs. Bottom right: construction of Dense Point Cloud.

As the flights were conducted with two UAVs equipped with different sensors with different characteristics, the spatial resolution (i.e pixel size) of each of the four DEMs was not the same. Hence, the DEMs pixel size had to be homogenized (7x7cm). For this purpose, ArcMap software was used and the resampling tool was applied with the nearest neighbour assignment technique, due to the type of data used. This process consists in unifying the pixel size by calculating how many cells of smaller size must be joined to create a pixel of larger size.

The most important topographic variables (slope, aspect, solar radiation) for calculating the rock surface temperature were derived from the DEM of each intertidal area. Aspect, slope and solar area were constructed in Environmental Systems Research Institute's (ESRI's) ArcMap 10.3 software, using the Spatial Analyst tool. The aspect is defined as the orientation of the slope, measured clockwise in degrees from 0 to 360, where 0 is north-facing, 90 is east-facing, 180 is south-facing, and 270 is west-facing. The slope was expressed in percentage of rise of the rocky surface. Solar area was calculated using the solar radiation tool, this allowed to know the insolation received by each of the rocky intertidal. The data was obtained in units of watt hours per square meter (Wh/m^2), and only for the hours where the study areas were not covered by water masses were selected. The time configuration was Multiple days in a year, selecting the days when UAVs flights were performed.

From the logger data, emersion time intervals and temperature values of the rock surface were acquired. A Pearson correlation analysis was performed using R software to determine the relationship between the rock surface temperature and the emersion time. Only the values from the shore surface were used, without the influence of sea water temperature. To obtain these values, the tidal height data from the nearest port of Viana do Castelo were compared with the data obtained from the loggers. They were filtered by time and tidal coefficients to get values for each of the points of the logger locations on emersion time. With the emersion time data, the maximum and minimum of each of the loggers were selected to obtain the thermal extremes of each of the points. All this treatment was done after the data from the loggers were selected to the same dates of the UAVs flights.

The values of the topographic variables were extracted for the location of each logger. All these processes (resample, merge, extract) were performed in ArcMap 10.3 software. The rock surface temperature data obtained by the loggers were selected and adjusted to have the same time interval in all study areas. To build a temperature surface model, a linear regression was used to calculate the mathematical model that best described the relation between the maximum and minimum temperature measured by loggers and topographic variables. This was performed using

R software and the raster package. The resulting mathematical model was then projected to the entire study area.

Lastly, to check how reliable the model built was, logger temperatures were compared to model predicted temperatures. To test if there were significant differences between measured and predicted temperatures a Wilcoxon test was applied.

3. Results

3.1 UAVs performance

Each of the intertidal areas (Carruagem, São Bartolomeu, Moinhos and Apúlia) was flown over under similar weather conditions. A total of 1141 pictures were taken in the four locations and 38 ground control points (GCPs) were collected over the whole intertidal area (Table 4). The total area surveyed covers a total of 80.459 m^2 of rocky intertidal. In the intertidal zones of Apúlia and São Bartolomeu, the height of the flights exceeded 31 meters, while in Carruagem and Moinhos, the average height of the flight was 20 meters (Fig. 7).

Figure 7: Two images of the flights. In the left, picture taken with UAVs FIMi X8 SE and on the right, picture taken with Phantom 4 - Pro.

Table 4: UAVs' rocky intertidal campaigns features. UAV: unmanned aerial vehicle; GCPs: ground control points.

STUDY AREA	UAV	CAMERA RESOLUTION	IMAGES	GCPS	PIXEL SIZE (m)
CARRUAGEM	DJI PHANTOM 4-PRO	20 Mp	246	12	0.036
SÃO BARTOLOMEU	XIAOMI FIMI X8 SE	12 Mp	252	6	0.07
MOINHOS	DJI PHANTOM 4-PRO	20 Mp	427	12	0.031
APÚLIA	XIAOMI FIMI X8 SE	12 Mp	216	8	0.032

3.2 Digital Elevation Models (DEM)

The DEM with higher spatial resolution was derived for the intertidal area of Moinhos (~0.031 m), while the DEM of the intertidal of São Bartolomeu had a value of 0.07 meters. The DEMs of the intertidal of Apúlia and Carruagem had a pixel size of 0.032 and 0.036 metres, respectively. The maximum elevation in the coastal area of Moinhos and São Bartolomeu was 13.5 and 13 meters, respectively, above mean sea level (Fig. 8). On the other hand, the maximum elevation in the coastal area of Carruagem and Apúlia was 8.33 meters and 9.33 meters, respectively, above mean sea level (Fig. 10). The coastal area with the lowest elevation was Moinhos -3,2 metres (Fig. 8). The coastal area of Carruagem, São Bartolomeu and Apúlia had negative elevations of -1.9, -2.13 and -2.31 metres, respectively (Fig.8).

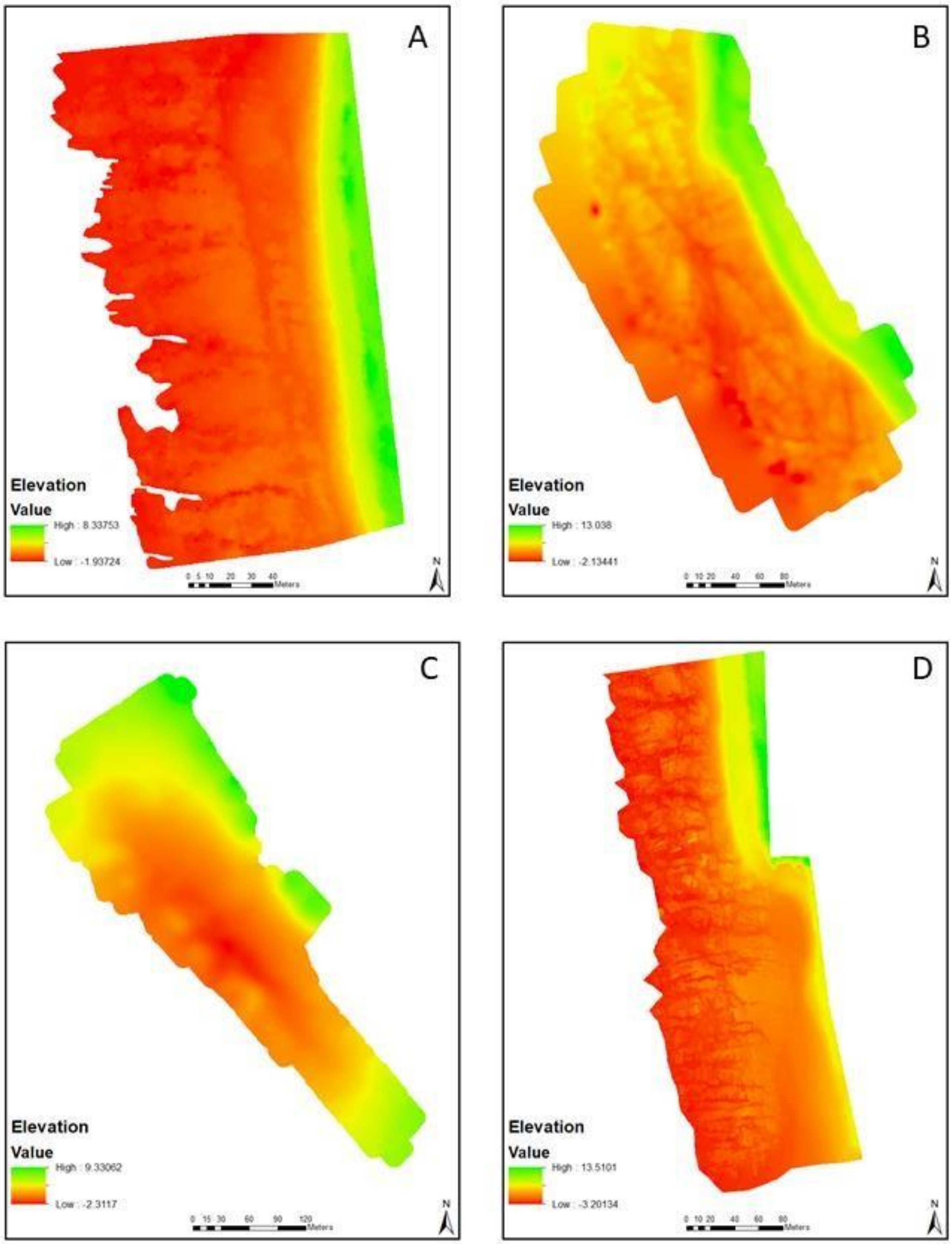

Figure 8: Composition of four Digital Elevation models (DEMs) for each intertidal area. A corresponds to th e DEM of Carruagem. B corresponds to the DEM of São Bartolomeu. C corresponds to the DEM of Apulia rocky shore and D corresponds to the DEM of Moinhos.

3.3 DEMs' products

The São Bartolomeu intertidal was the only one with aspect values between -1º and 359.9º. Aspect values equal to -1º correspond to flat areas. On the contrary, the intertidal of Apúlia had aspect values between 0º and 359.9º, the intertidal of Moinhos had values between 0.18º and 359.8º and finally the intertidal of Carruagem has aspect values between 0.001º and 359.9º.

The intertidal of Apúlia showed less variation of aspect with a prenominal orientation to south, the areas of São Bartolomeu, Carruagem and Moinhos were highly variable (Fig. 9, Fig. 10, Fig. 11). The slope of the intertidal of São Bartolomeu ranged between 0 and 80.8 % (Fig. 10). Comparing with the remaining intertidal areas, it had the highest slope. In the intertidal of Apúlia the slope values ranged from 0.004 to 78.9 %, in Carruagem from 0 to 80 % and finally in the intertidal of Moinhos from 0.18 to 80.1 %.

The solar radiation in Apúlia was 150388 Wh/m^2 and in Moinhos 151332 Wh/m^2, being these the two intertidal areas with the highest radiation (Fig. 12). The intertidal areas of São Bartolomeu (148737 Wh/m^2) and Carruagem (145444 Wh/m^2) were the areas with the lowest values of solar radiation (Fig. 10).

The maximum temperature collected by loggers in the selected period ranged between 16.2 - 21.7 °C, 18.9 - 34.2 °C, 18.3 - 26.1 °C for Carruagem, Moinhos and Apúlia, respectively (Table 5). The minimum temperature ranged between 10.3 - 12 °C, 4.7 - 6.4 °C and 9.1 - 9.7 °C in Carruagem, Moinhos and Apúlia, respectively.

In the location of each logger, aspect ranged within each location: 184.2º - 327.3º for Carruagem, 17.4º - 0 343º for Moinhos and 84.8º - 90º for Apúlia (Table 5). Slope varied between 0.8 - 8.8 % in Carruagem, 12.4 - 75.6 % in Moinhos and 3.2 - 3.4 % in Apúlia (Table 5). Solar radiation was measured between 76848 and 95459.6 Wh/m^2 in Carruagem, 17210.8 and 141319 Wh/m^2 in Moinhos and 92602.6 and 93188.8 Wh/m^2 in Apúlia (Table 5).

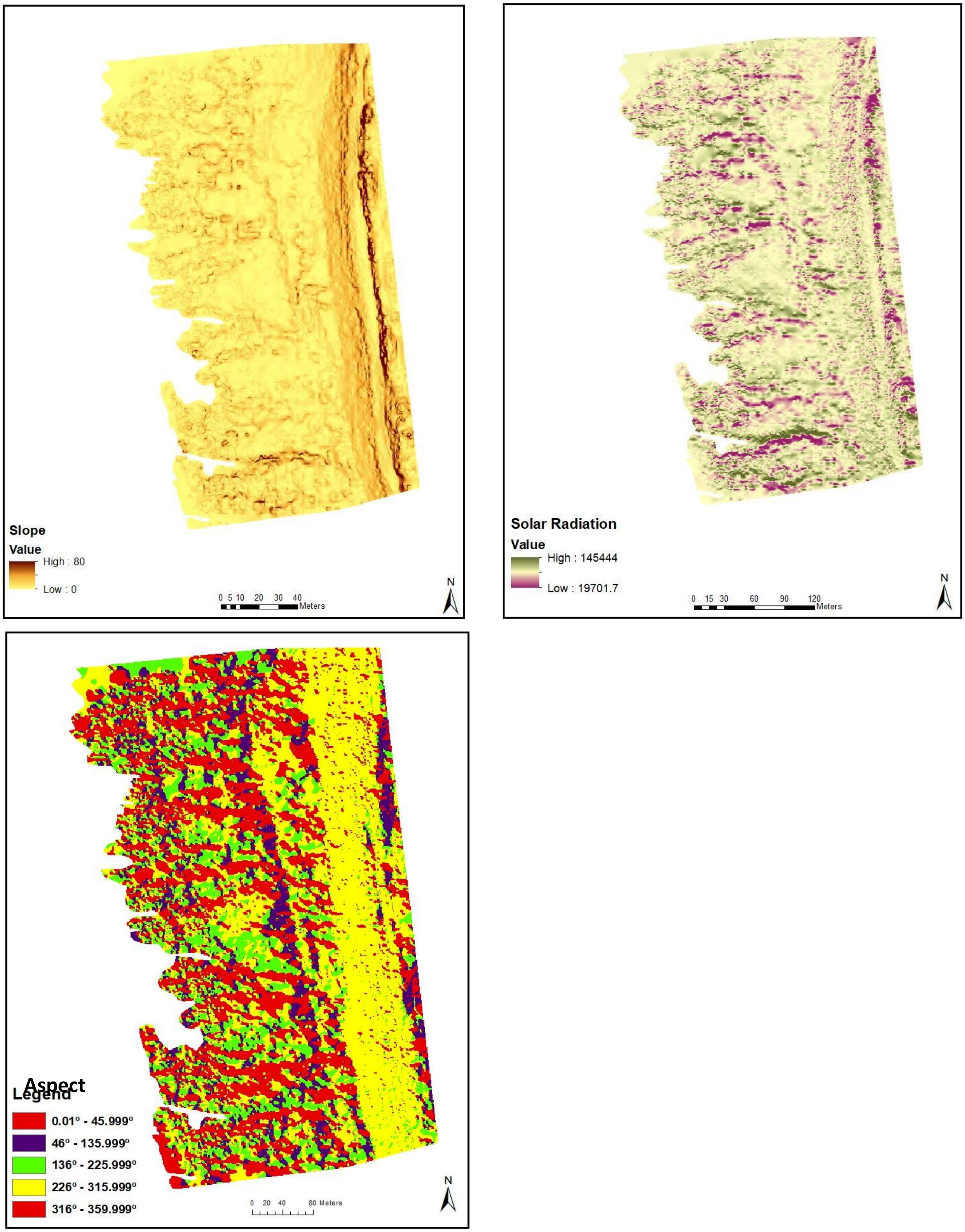

Figure 9: Composition of topographic variables of the intertidal of Carruagem.

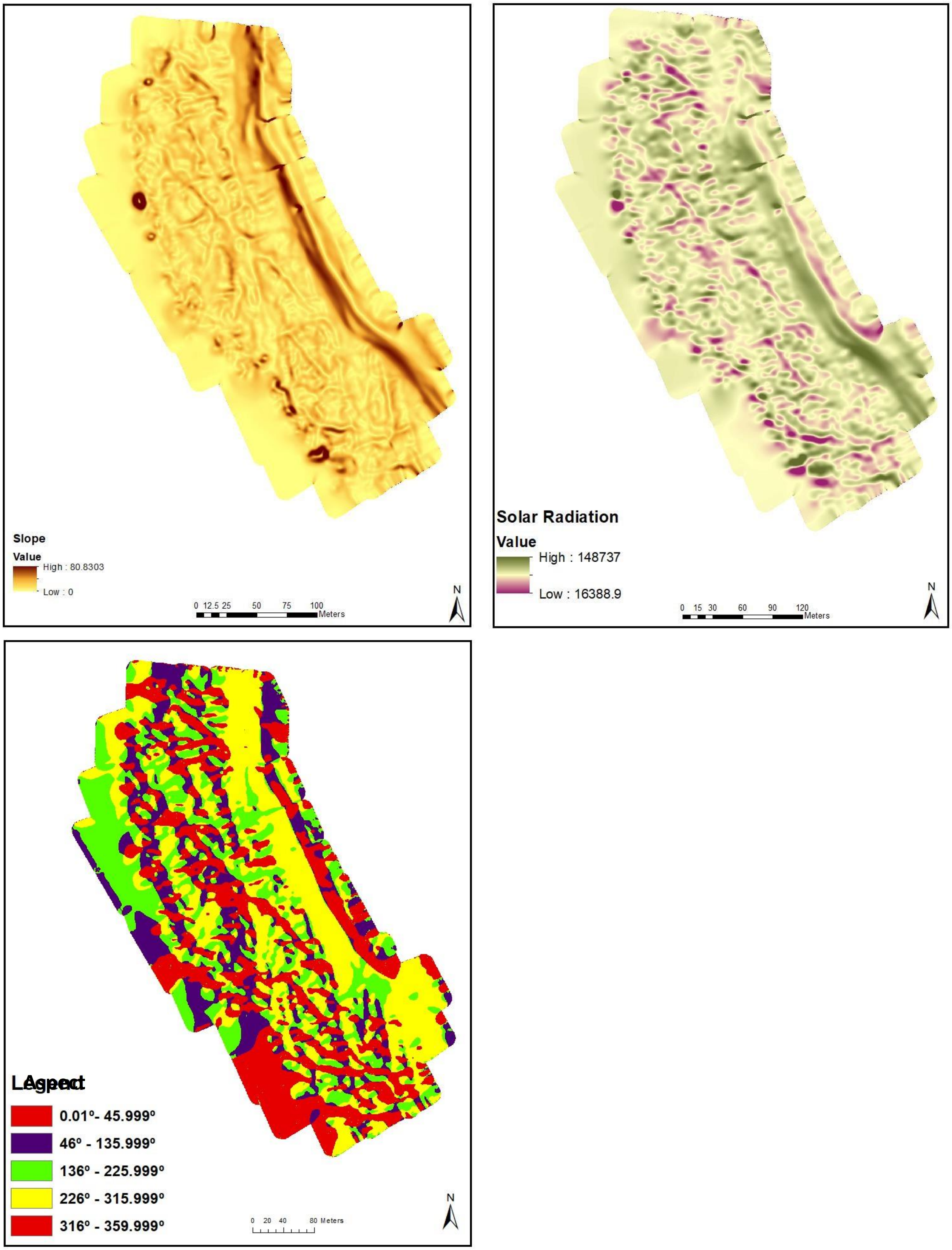

Figure 10: Composition of topographic variables of the intertidal of São Bartolomeu.

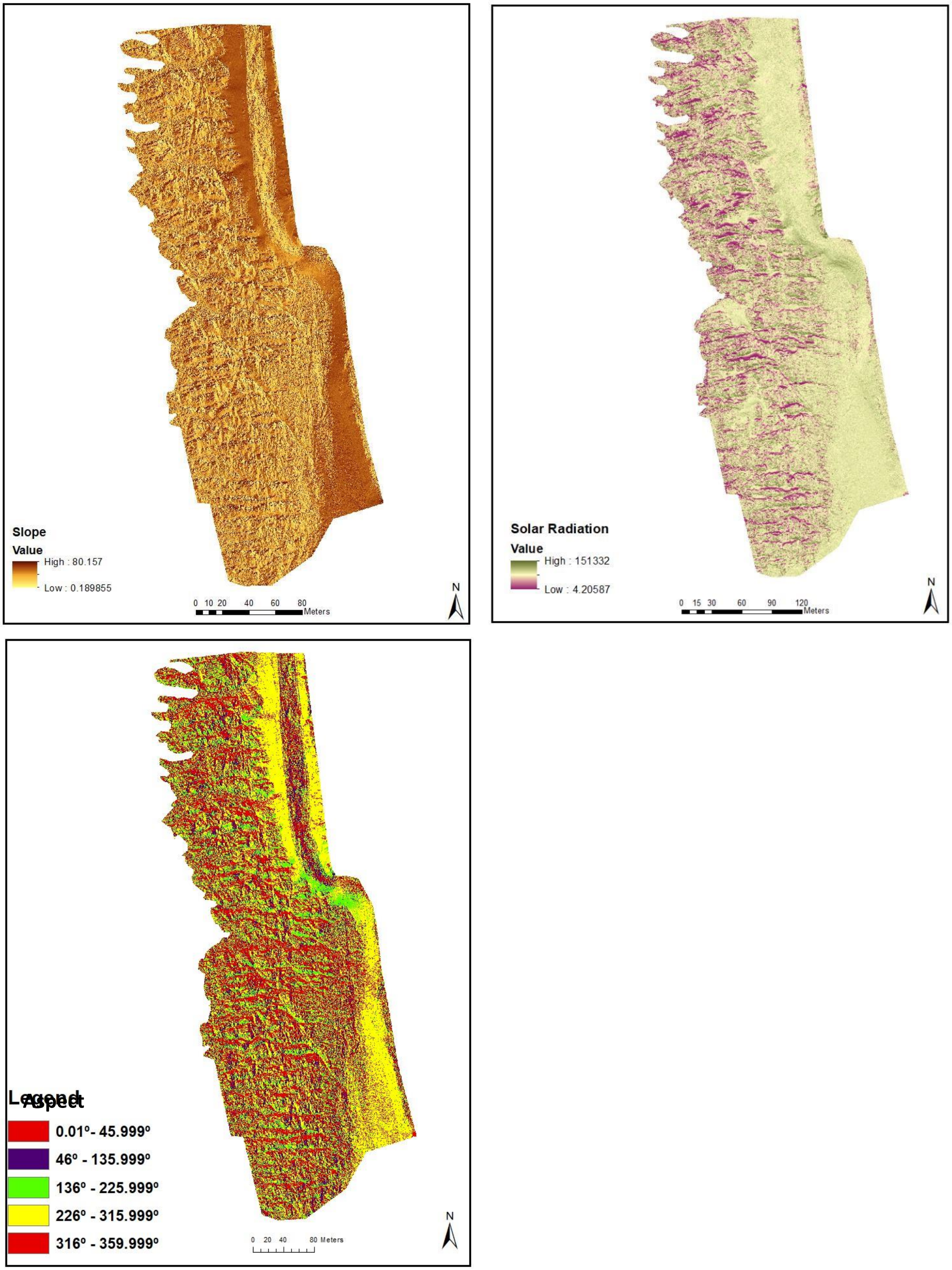

Figure 11: Composition of topographic variables of the intertidal of Moinhos.

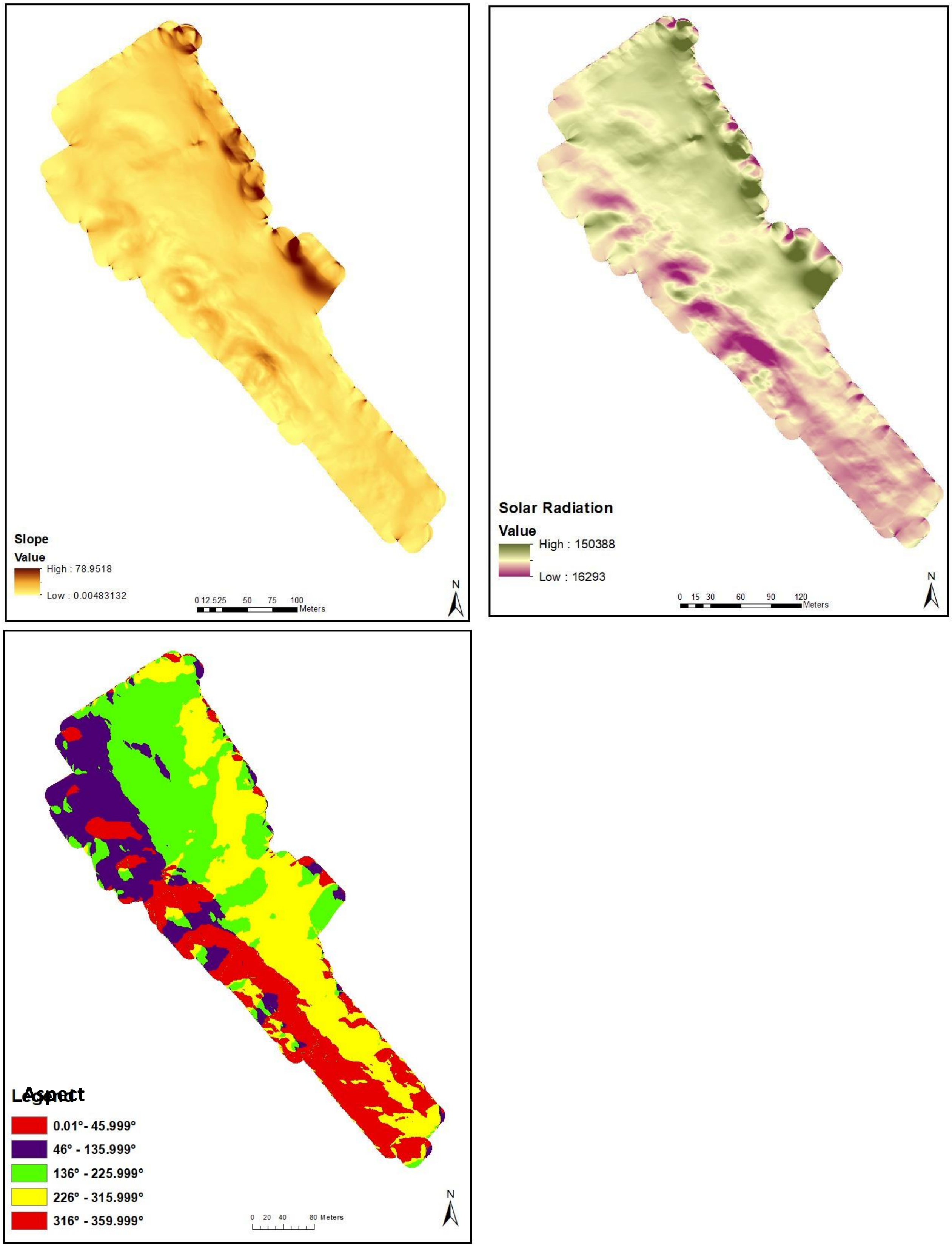

Figure 12: Composition of topographic variables of the intertidal of Apulia.

Table 5: The exact location of each of the loggers and the coefficients of the extracted topographic variables.

LOGGER X_UTM29 (m)	LOGGER Y_UTM29 (m)	ASPECT (º)	SLOPE (%)	SOLAR RADIATION (wh/m²)	ROCKY SURFACE TEMPERATURE MAX. (°C)	ROCKY SURFACE TEMPERATURE MIN. (°C)	ROCKY INTERTIDAL
516031.9	4605020.2	184.2	0.8	93456.0	21.7	11.2	Carruagem
516032.5	4605024.1	262.6	2.8	92380.1	17.8	10.3	Carruagem
516032.6	4605022.2	218.0	2.4	95459.6	27.0	10.8	Carruagem
516032.3	4605022.6	327.3	8.8	76848.0	16.2	12.0	Carruagem
516871.6	4601724.7	36.45	72.1	17210.8	19.3	6.1	Moinhos
516874.1	4601724.5	343.3	69.6	17969.7	20.3	5.9	Moinhos
516871.7	4601724.6	17.4	75.6	20647.6	18.9	6.4	Moinhos
516869.6	4601721.2	202.8	12.4	114183.0	31.6	5.0	Moinhos
516873.7	4601720.3	214.5	24.6	124375.0	34.2	5.2	Moinhos
516871.6	4601720.9	180.1	32.8	141319.0	31.3	4.7	Moinhos
517983.1	4592994.5	84.8	3.3	92602.6	26.1	9.5	Apulia
517983.3	4592994.7	86.8	3.4	92812.1	18.3	9.6	Apulia
517985.1	4592994.1	89.6	3.3	93140.0	23.0	9.1	Apulia
517985.3	4592994.3	90.0	3.2	93188.8	18.8	9.7	Apulia

3.4 Rock surface temperature model

Two models were derived to create a minimum and maximum temperature rock surface model. Pearson correlation test showed that temperature was highly correlated to emersion time. For this reason data from the loggers corresponding to emersion time were not used. The model created with the minimum temperatures recorded by the loggers and the topographic variables was statistically significant. The most relevant variables for this model were Aspect and Slope explain 87% of the variability of the temperature (R^2 = 0,87) (Table 6). The result created for the model with maximum temperatures recorded by the loggers and the topographic variables was also statistically significant. For this model the most relevant variables were Slope and Solar Radiation which explain 75% of the variability of the temperature (R^2 = 0,75) (Table 7). The values obtained from the two models were similar to the ones recorded by the loggers (Table 8). The maximum temperature predicted was 36.8 ºC in the intertidal of Moinhos (Fig. 17). The minimum temperature was also in the intertidal of Moinhos with a value of 3.9 ºC (Fig. 18). The rock surface temperature values measured by all the loggers and the minimum and maximum temperature values predicted by the models were not statistically different (Wilcoxon test: V= 55, p = 0.90).

Table 6: Summary of results of the Minimum Surface Temperature Model. Significance code: p-value, *** [0, 0.001], ** (0.001, 0.01],* (0.01, 0.05], . (0.05, 0.1], (0.1, 1].

	Estimate	Std. Error	T value	Pr(>ItI)
ASPECT	7.539e-01	1.520e-01	4.961	0.00057 ***
SLOPE	2.662e-02	2.844e-03	-9.359	2.91e-06 ***
SOLAR RADIATION	8.976e-07	9.322e-06	-0.096	0.92519
RESIDUAL STANDARD ERROR	0.9284 on 10 degrees of freedom			
MULTIPLE R-SQUARED	0.9007, Adjusted R-squared: 0.8709			
F-STATISTIC	30.24 on 3 and 10 DF, p-value: 2.503e-05			

Table 7: Summary of results of the Maximum Surface Temperature Model. Significance code: p-value, *** [0, 0.001], ** (0.001, 0.01],* (0.01, 0.05], . (0.05, 0.1], (0.1, 1]

	Estimate	Std. Error	T value	Pr(>ItI)
ASPECT	-1.0637947	0.4776500	-2.227	0.050085
SLOPE	0.0429849	0.0089387	4.809	0.000714 ***
SOLAR RADIATION	0.0001454	0.0000293	4.962	0.000568 ***
RESIDUAL STANDARD ERROR	2.918 on 10 degrees of freedom			
MULTIPLE R-SQUARED	0.8091, Adjusted R-squared: 0.7518			
F-STATISTIC	14.13 on 3 and 10 DF, p-value: 0.0006291			

Table 8: Data of the rocky surface measured for the loggers and rocky surface predict with the model.

X_UTM29 (m)	Y_UTM29 (m)	TEMPERATURE LOGGERS MIN. (ºC)	TEMPERATURE PREDICT MIN. (ºC)	TEMPERATURE LOGGERS MAX. (ºC)	TEMPERATURE PREDICT MAX. (ºC)	ROCKY INTERTIDAL
516871.7	4601724.8	6.1	7.1	19.3	18.5	Moinhos
516874.1	4601724.6	5.9	4.9	20.3	20.4	Moinhos
516871.7	4601724.7	6.4	7.1	18.9	18.5	Moinhos
516869.7	4601721.2	5	5.5	31.6	32.2	Moinhos
516873.8	4601720.3	5.2	5.2	34.2	32.7	Moinhos
516871.7	4601720.9	4.7	5.3	31.3	32.1	Moinhos
517983.1	4592994.5	9.5	8.9	26.1	22.6	Apulia
517983.3	4592994.7	9.6	8.9	18.3	22.7	Apulia
517985.1	4592994.1	9.6	8.9	23	22.7	Apulia
517985.3	4592994.3	9.7	8.9	18.8	22.7	Apulia
516031.9	4605020.2	11.2	10.5	21.7	20.5	Carruagem
516032.5	4605024.1	10.3	11.9	17.8	18.3	Carruagem
516032.6	4605022.2	10.8	10.4	27	27.7	Carruagem
516032.3	4605022.6	12	11.9	16.2	18.3	Carruagem

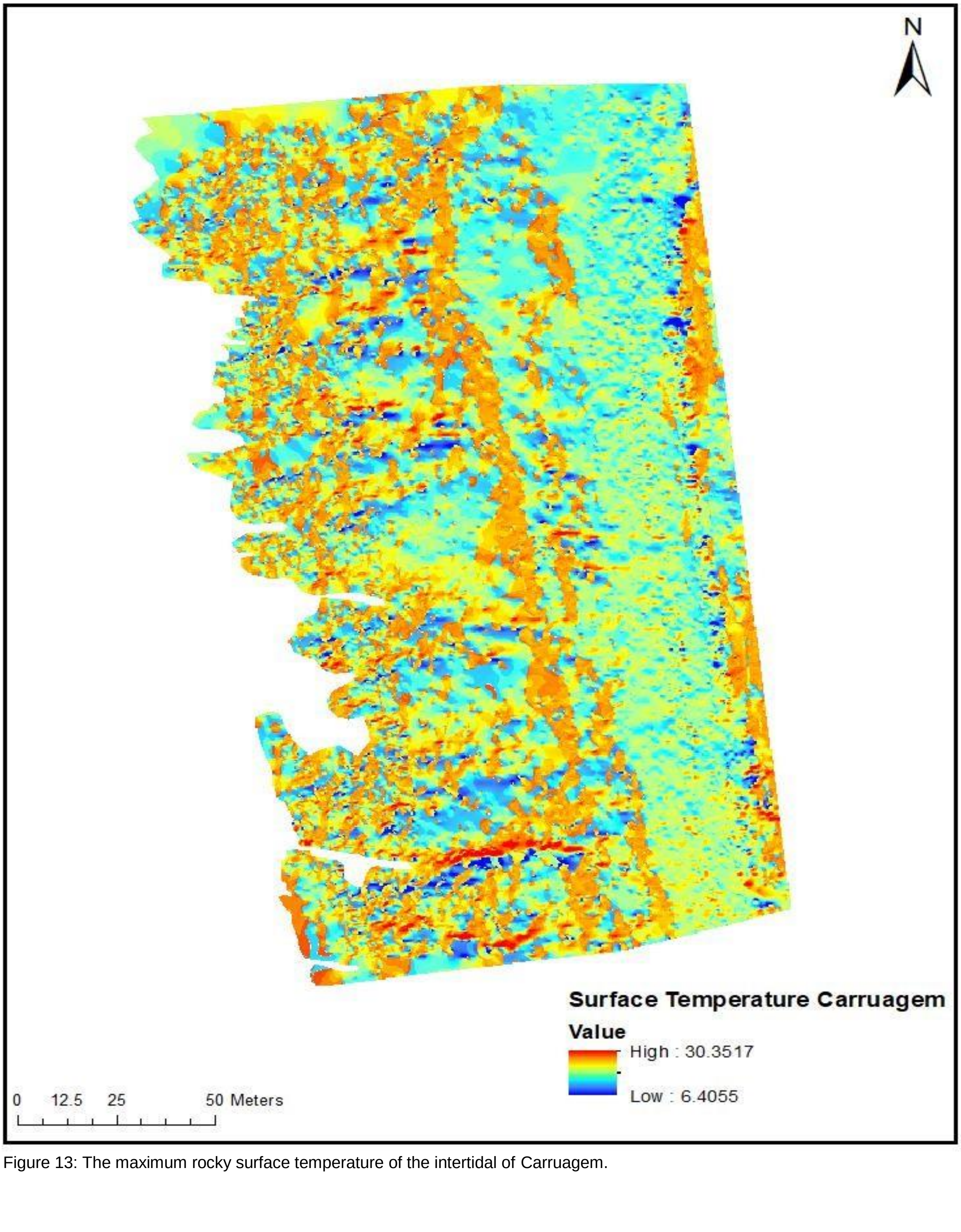

Figure 13: The maximum rocky surface temperature of the intertidal of Carruagem.

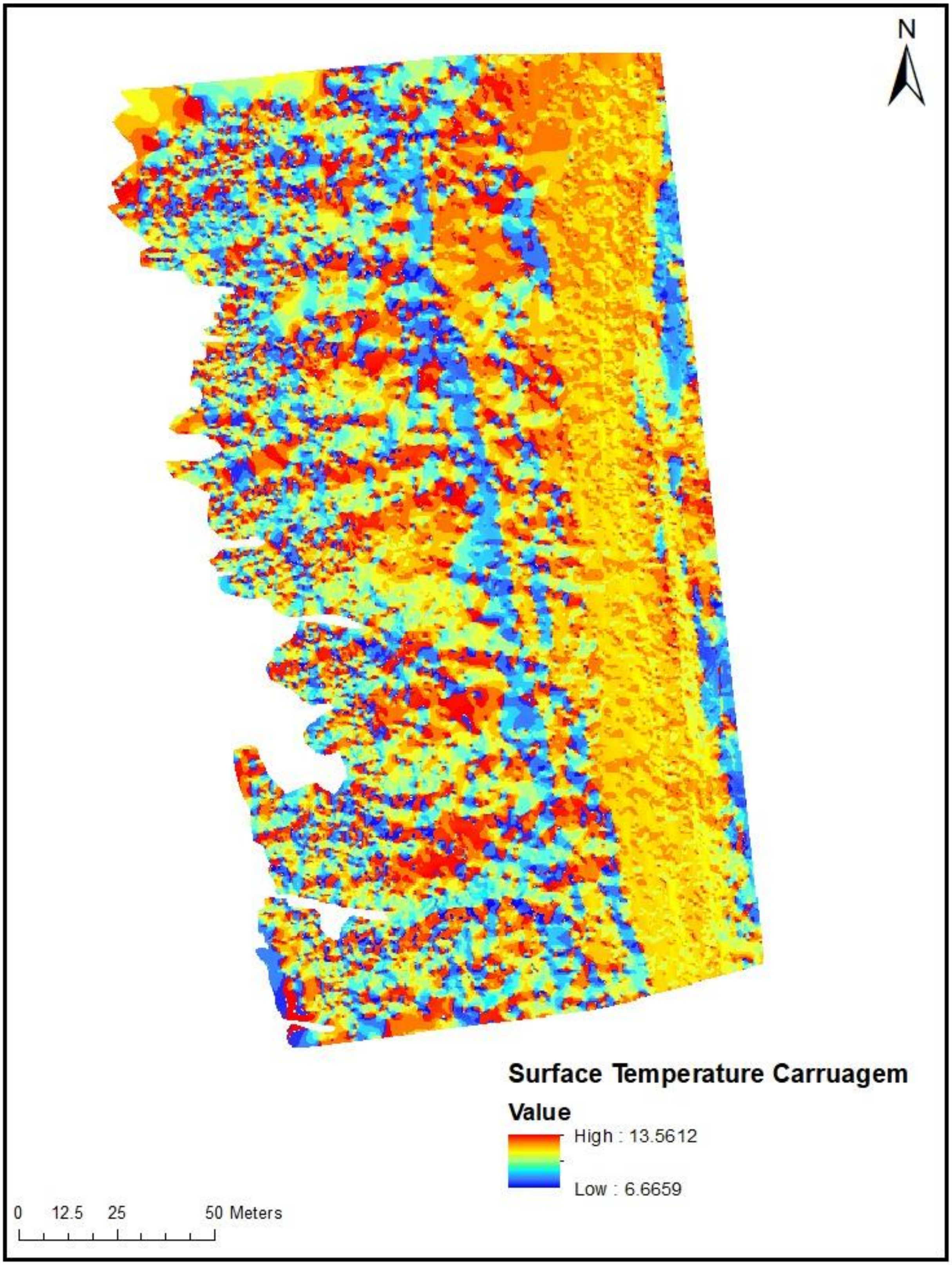

Figure 14: The minimum rocky surface temperature of the intertidal of Carruagem.

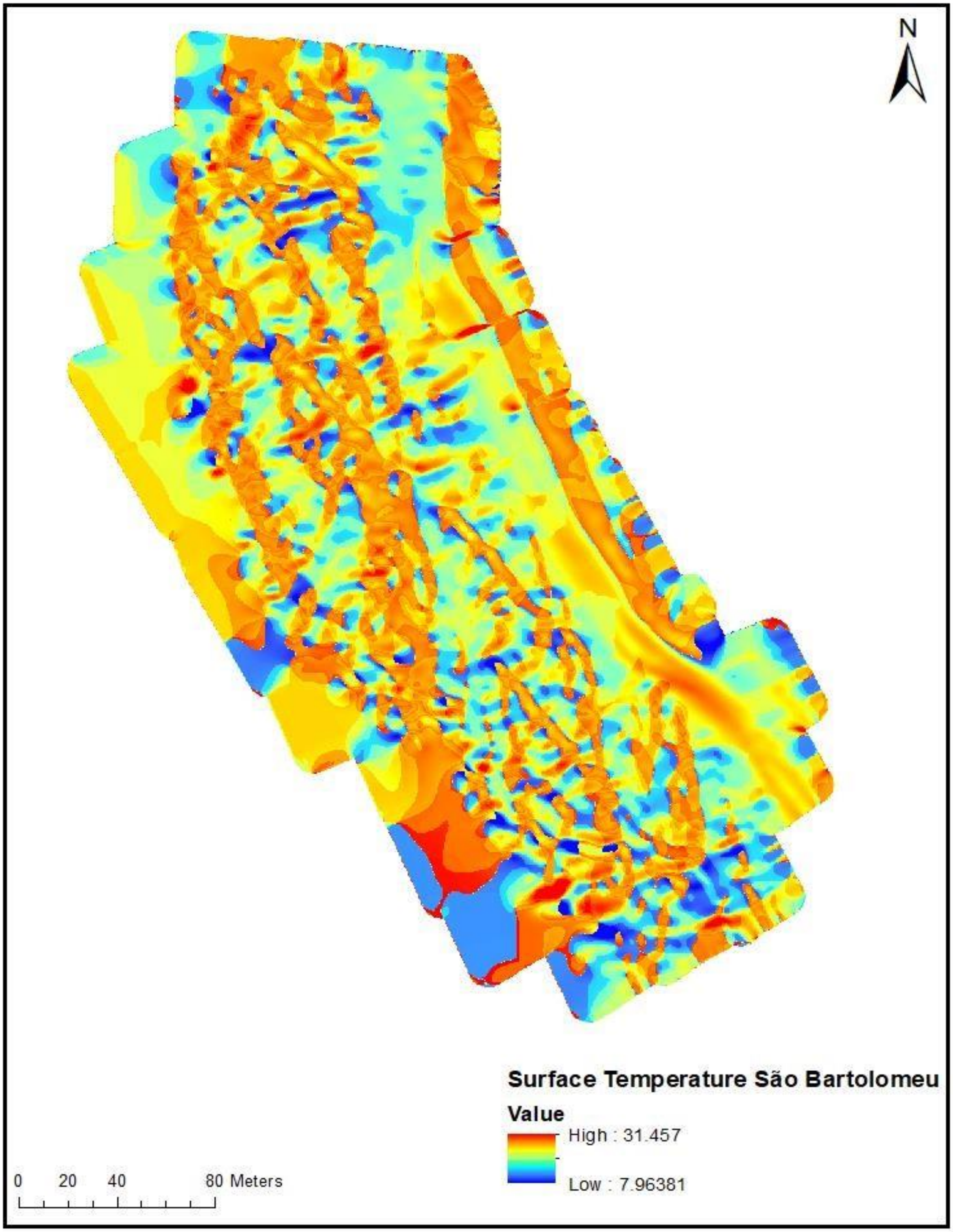

Figure 15: The maximum rocky surface temperature of the intertidal of São Bartolomeu.

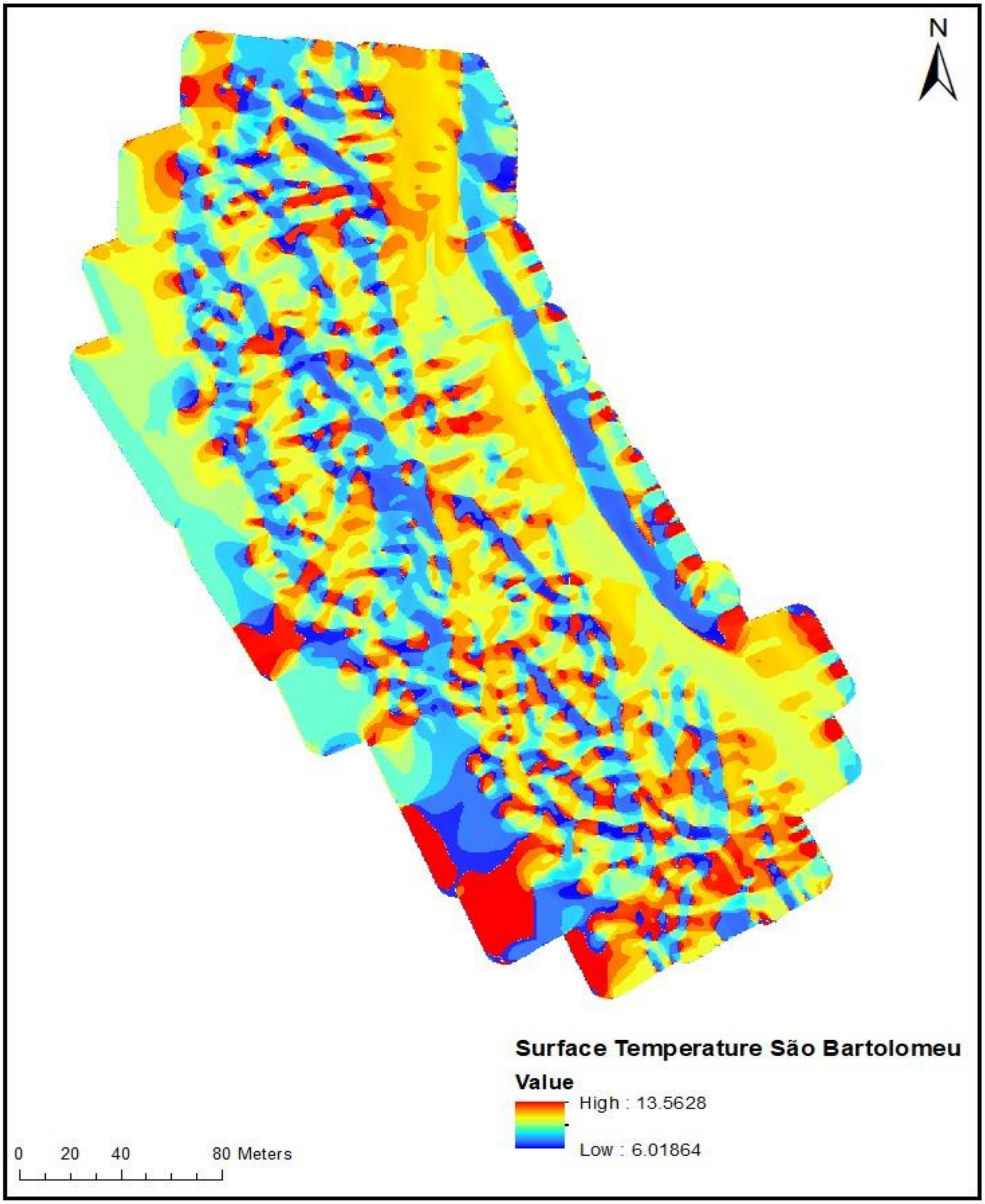

Figure 16: The minimum rocky surface temperature of the intertidal of São Bartolomeu.

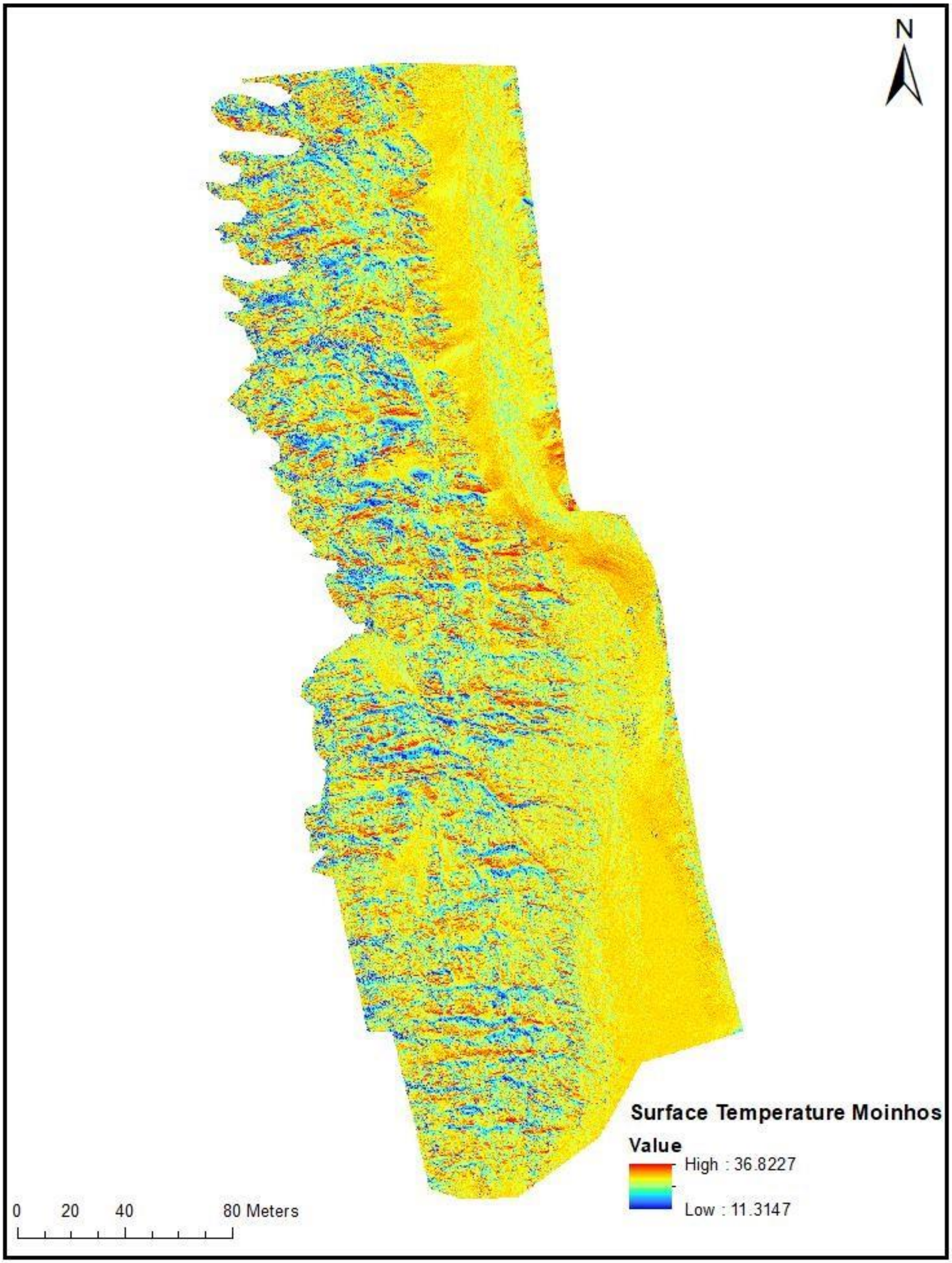

Figure 17: The maximum rocky surface temperature of the intertidal of Moinhos.

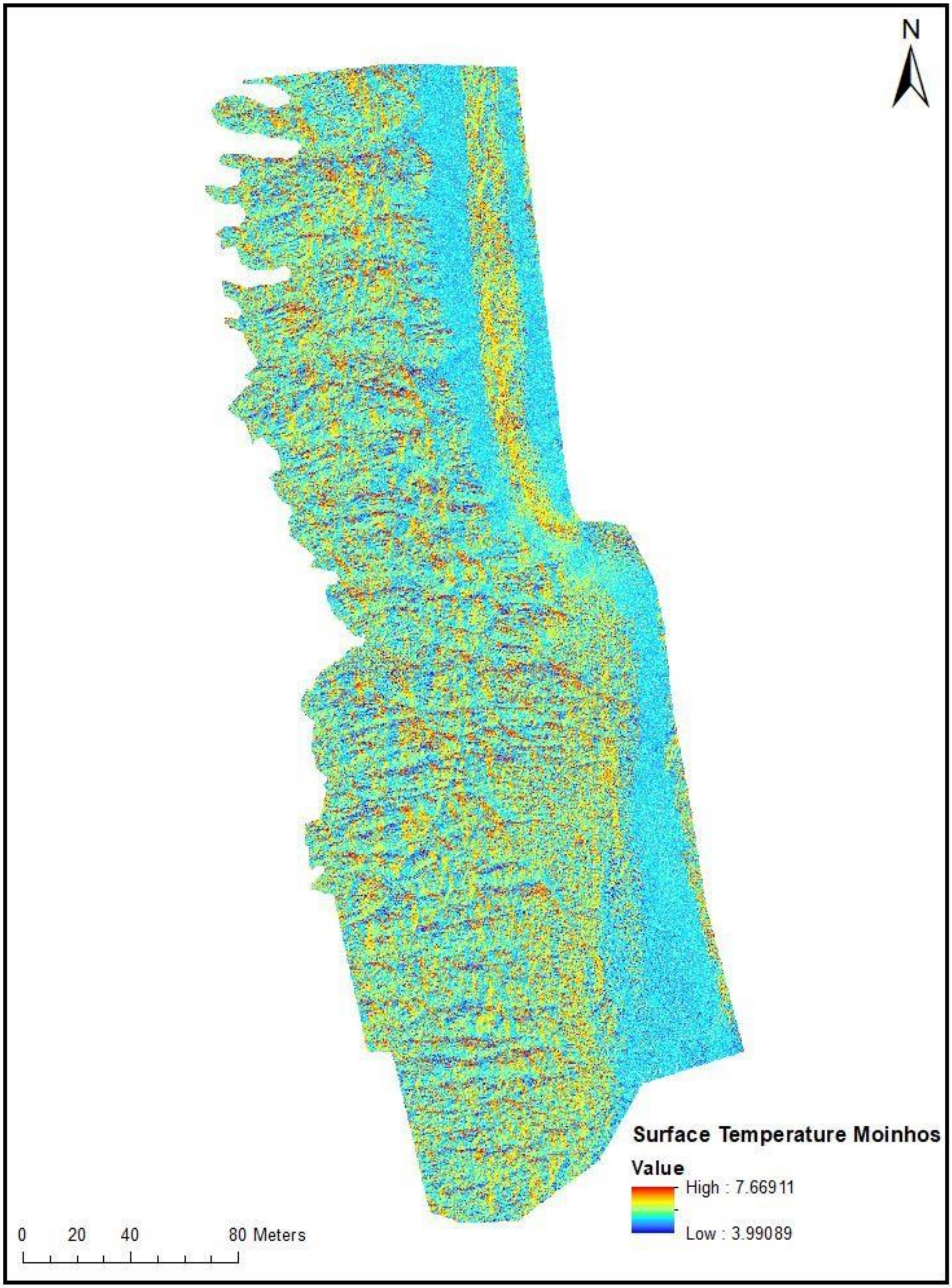

Figure 18: The minimum rocky surface temperature of the intertidal of Moinhos.

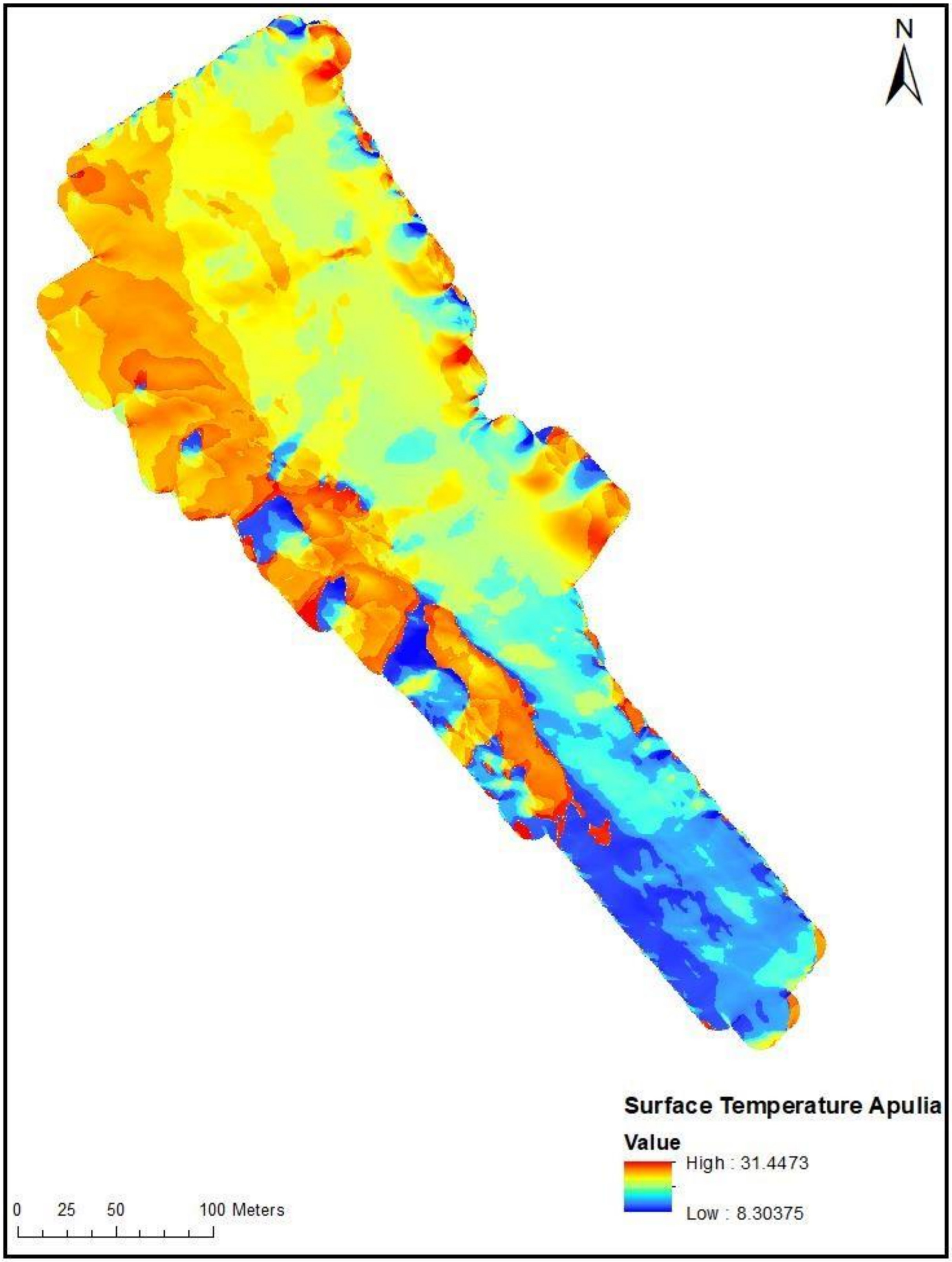

Figure 19: The maximum rocky surface temperature of the intertidal of Apulia.

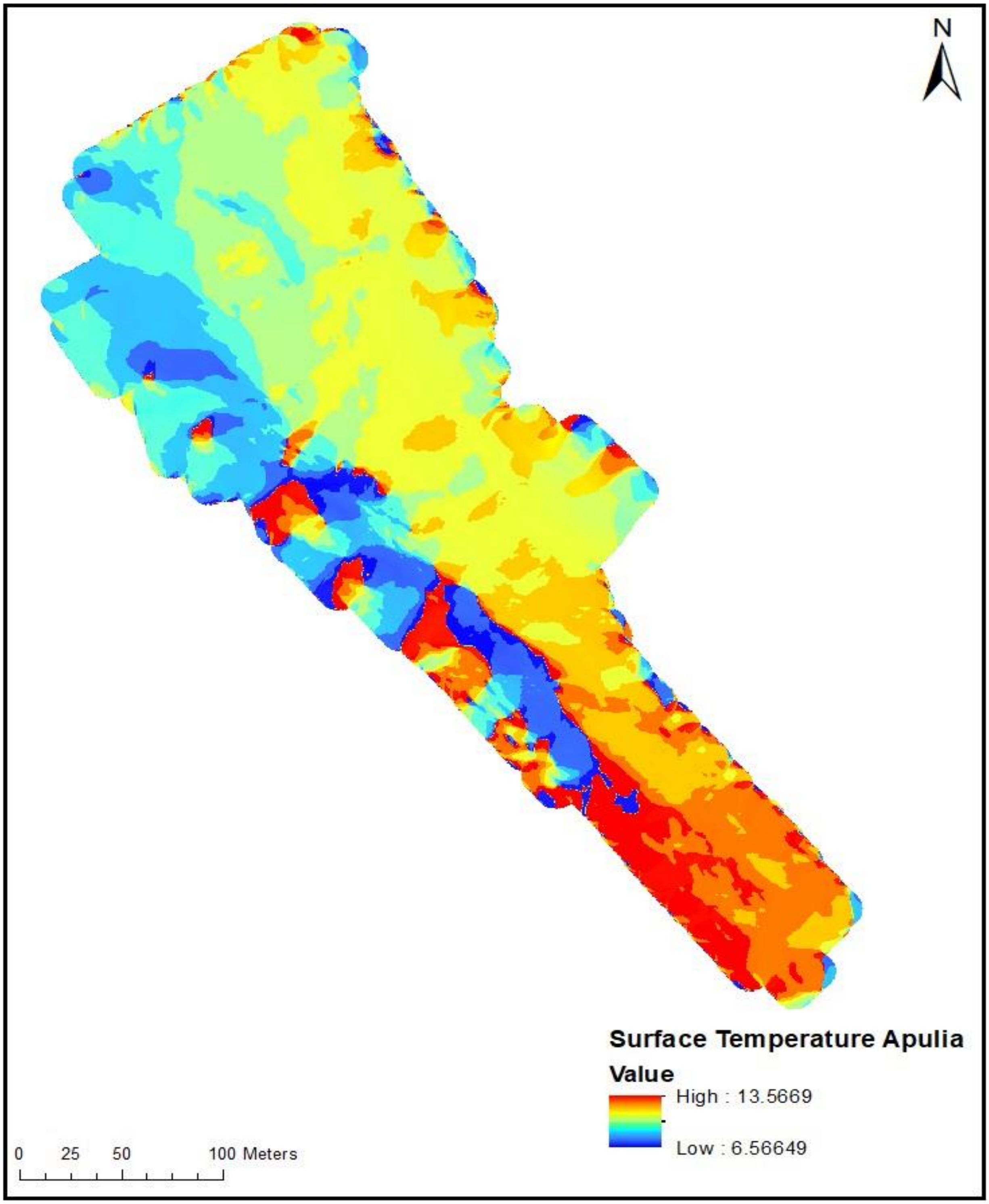

Figure 20: The minimum rocky surface temperature of the intertidal of Apulia

4. Discussion and future projections

This thesis aims to to build topographic maps of four intertidal rocky shores of PNLN, based on flights done by UAVs and to create a surface temperature model from derived topographic products of the Digital elevation model (DEM) together with physical data collected in situ (loggers). For this, DEMs were built for four rocky shores of Parque Natural do Litoral Norte. The pixel size of the four DEMs ranged between 3 and 8 centimeters what is in accordance with other works (Dai et al., 2018). The resolution of the DEMs was affected by the height at which the flights were performed, and the resolution of the camera attached to the drone. Indeed, Leitão et al., (2016) has also observed the effect of the flight height and camera resolution in the resolution of their DEMs. As expected, the higher values of altitude correspond to dunes or boulders, mainly present in the intertidal of Moinhos and São Bartolomeu (Fig. 10) The intertidal of São Bartolomeu and Apúlia are oriented to the north in most of their extension, making them the shores with more cold spots. They are also the two rocky shores with more flat areas, which are more susceptible to temperature changes, cooling down faster (Janetzki et al., 2021). Carruagem and Moinhos are oriented towards the west, making them the coastal areas with the higher values of solar radiation. The intertidal of Moinhos has a high elevation compared to the other areas and showed the highest levels of solar radiation. In the intertidal of Moinhos, the largest range of temperatures can be observed due to its steep slope and the orientation. The two other intertidal sites, Apúlia and Carruagem, were found more uniform, having less variation in slope and aspect. Therefore, a smaller temperature range was observed.

In this work, 80495 m^2 were mapped and temperature values were predicted for this entire area using fourteen loggers. The position where the loggers were placed plays a fundamental role in characterizing the different thermal levels present in the intertidal (Reid & Harley, 2021). Maximum and minimum temperature data recorded at the rock surface yielded surprising results, with temperature variations of more than 29 ºC having been recorded. These data revealed that temperature variations within these rocky areas are far wider than previously believed from studies using data obtained from nearby weather stations or satellite data (Jurgens & Gaylord, 2018; J. Lathlean et al., 2011; J. A. Lathlean et al., 2014). This is particularly important as the highest mortality events of the organisms that inhabit the rocky intertidal occur from both high and low temperature peaks during aerial exposure (Harley, 2008; Nielsen et al., 2021; Wethey et al., 2011). On the other hand, the number of loggers is a key factor to rigorously determine all the different temperatures in locations such an irregular terrain as the intertidal (H.-Y. Wang et al., 2020). Models of the minimum and maximum surface temperature were build using data from these fourteen loggers. The rocky shore of São Bartolomeu had no loggers installed, and so it was used as an area to test if the predicted models were accurate. Although the sample size is very low, models explained high percentage of variability of the observed temperature (Minimum Surface Temperature Model - $R^2 = 0.87$, Maximum Surface Temperature Model – $R^2 = 0.75$). Despite the low number of loggers, the models were able to predict both minimum and maximum temperature for the locations of loggers (Wilcoxon test, $p>0.05$). Although they are very accurate in training data prediction, there should be some uncertainty when predicting to the entire study area. Indeed, most spatial modelling studies that aim to predict a physical variable such as temperature, whether of the rock surface, air or sea, usually involve greater amounts of loggers, meteorological stations or satellite imagery (Gandra et al., 2015; Maclean et al., 2019; Seabra et al., 2011; M. Wang et al., 2017). Further work will be done to improve both model predictions and validation. For this, data from other locations, further away from the ones used so far, will be obtained by implementing more loggers. This work consisted of an initial attempt to create a surface model, creating a methodology, that once further developed, can be applied in the future.

This thesis demonstrates that UAVs equipped with optical sensors capturing high-resolution images are a very valuable tool for developing topographic maps of rocky intertidal areas (Choi et al., 2019). The simplicity and pace with which UAVs capture data has been demonstrated in this work. This equipment is a powerful instrument for quantifying spatial patterns of organisms living in the rocky intertidal (Gomes et al., 2018). The complex geomorphology that was found in these rocky intertidal areas and the fact that they suffer tidal effects make them an ideal place for UAVs surveys. However, it remains a challenging job working with drones due to their vulnerability to fast changing weather conditions, such as, strong winds, rain and cloud coverage (Kellaris et al., 2019). Another conclusion of this work is that it is not easy to work with loggers placed in the rocky intertidal. The high dynamism that characterizes these areas added to various physical factors that alter the morphology of the rocky shores, difficult the finding of these equipments. It was challenging to extract data from each of them in the three shores and to clean the extracted data to have the aerial time intervals. However, to understand the behavior of the animals living on top of the rock, this kind of data is essential (Judge et al., 2018).

This work shows the great potential that UAVs have for the creation of high spatial resolution topographic maps, in places such as the intertidal. Biological data collected in situ combined with data from UAVs present a great opportunity to study spatial patterns of organisms that can be influenced by physical parameters (Helmuth et al., 2006). It is necessary to carry out more studies with UAVs in the intertidal to achieve monitoring, protection, and conservation plans. The models created are a first attempt, being the basis for further studies. In the future, a surface temperature model will be creating using high number of loggers. The model will be therefore improved and validated. It will be than used to related with biological data in order in climate change studies.

References

AgiSoft PhotoScan Standard (Version 1.2.6)

Anderson, K., & Gaston, K. J. (2013). Lightweight unmanned aerial vehicles will revolutionize spatial ecology. Frontiers in Ecology and the Environment, 11(3), 138–146. https://doi.org/10.1890/120150

Baena, S., Moat, J., Whaley, O., & Boyd, D. S. (2017). Identifying species from the air: UAVs and the very high resolution challenge for plant conservation. PLOS ONE, 12(11), e0188714.

https://doi.org/10.1371/JOURNAL.PONE.0188714

Bertocci, I., De Oliveira Martins, M. I., Meyer, H. S., Gómez, O. B., Maggi, E., & Arenas, F. (2021). Resurvey of sea urchins and mussels at protected and harvested shores a decade after: A beyond-BACI approach. Marine Environmental Research, 169, 105347. https://doi.org/10.1016/J.MARENVRES.2021.105347

Borges, D., Azevedo, I., Pádua, L., Adão, T., Peres, E., Sousa, J., Sousa Pinto, I., & Gonçalves, J. (2019). Mapping seaweed beds using multispectral imagery retrieved by unmanned aerial vehicles. Frontiers in Marine Science, 6, 28–29. https://doi.org/10.3389/conf.fmars.2019.08.00177

Choi, F., Gouhier, T., Lima, F., Rilov, G., Seabra, R., & Helmuth, B. (2019). Mapping physiology:

biophysical mechanisms define scales of climate change impacts. Conservation Physiology, 7(1), 1–18. https://doi.org/10.1093/conphys/coz028

Chuvieco, E. (2020). Fundamentals of Satellite Remote Sensing (Vol. 148). CRC Press. https://doi.org/10.1201/9780429506482

Colefax, A. P., Butcher, P. A., & Kelaher, B. P. (2018). The potential for unmanned aerial vehicles

(UAVs) to conduct marine fauna surveys in place of manned aircraft. ICES Journal of Marine Science, 75(1), 1–8. https://doi.org/10.1093/ICESJMS/FSX100

Colomina, I., & Molina, P. (2014). Unmanned aerial systems for photogrammetry and remote sensing: A review. ISPRS Journal of Photogrammetry and Remote Sensing, 92, 79–97.

https://doi.org/10.1016/J.ISPRSJPRS.2014.02.013

Cruzan, M. B., Weinstein, B. G., Grasty, M. R., Kohrn, B. F., Hendrickson, E. C., Arredondo, T.

M., & Thompson, P. G. (2016). Small unmanned aerial vehicles (micro-UAVs, drones) in

plant ecology. Applications in Plant Sciences, 4(9), 1600041. https://doi.org/10.3732/APPS.1600041

Dai, W., Li, H., Zhou, Z., Cybele, S., Lu, C., Zhao, K., Zhang, X., Yang, H., & Li, D. (2018). UAV

Photogrammetry for Elevation Monitoring of Intertidal Mudflats. Journal of Coastal Research, 85(85 (10085)), 236–240. https://doi.org/10.2112/SI85-048.1

Escobar-Sánchez, G., Haseler, M., Oppelt, N., & Schernewski, G. (2021). Efficiency of Aerial

Drones for Macrolitter Monitoring on Baltic Sea Beaches. Frontiers in Environmental Science, 0, 283. https://doi.org/10.3389/FENVS.2020.560237

Faria, S. C., Bianchini, A., Lauer, M. M., Zimbardi, A. L. R. L., Tapella, F., Romero, M. C., &

McNamara, J. C. (2020). Living on the Edge: Physiological and Kinetic Trade-Offs Shape Thermal Tolerance in Intertidal Crabs From Tropical to Sub-Antarctic South America.

Frontiers in Physiology, 11, 312.

Fitzhenry, T., Halpin, P. M., & Helmuth, B. (2004). Testing the effects of wave exposure, site, and behavior on intertidal mussel body temperatures: applications and limits of temperature logger design. Marine Biology 2004 145:2, 145(2), 339–349. https://doi.org/10.1007/S00227004-1318-6

Gandra, M., Seabra, R., & Lima, F. P. (2015). A low-cost, versatile data logging system for ecological applications. Limnology and Oceanography: Methods, 13(3), 115–126. https://doi.org/10.1002/LOM3.10012

Garza, C. (2016). Landscape Complexity Effects on Fisheries: Insights from Marine Landscape

Ecology. Current Landscape Ecology Reports 2016 1:1, 1(1), 1–9. https://doi.org/10.1007/S40823-016-0003-Z

Geologia | Hidrologia | Clima — ICNF. (n.d.). Retrieved August 10, 2021, from http://www2.icnf.pt/portal/ap/p-nat/pnln/geo

Gonçalves, J. A., Bastos, L., Madeira, S., Magalhães, A., & Bio, A. (2018). Three-dimensional data collection for coastal management – efficiency and applicability of terrestrial and airborne methods. International Journal of Remote Sensing, 39(24), 9380–9399. https://doi.org/10.1080/01431161.2018.1523591

Hawkins, S. J., Pack, K. E., Firth, L. B., Mieskowska, N., Evans, A. J., Martins, G. M., Aberg, P.,

Adams, L. C., Arenas, F., & Boaventura, D. M. (2019). The intertidal zone of the North-East Atlantic region: pattern and process.

ICNF. (2018). Paisagem Protegida Regional do Litoral de Vila do Conde e Reserva Ornitológica de Mindelo. Instituto de La Conservación de La Naturaleza y de Los Bosques. http://www2.icnf.pt/portal/ap/amb-reg-loc/pais-proteg-reg-lit-vila-conde-e-res-ornit-mindelo

Janetzki, N., Benkendorff, K., & Fairweather, P. G. (2021). Rocks of different mineralogy show different temperature characteristics: implications for biodiversity on rocky seashores. PeerJ, 9, e10712. https://doi.org/10.7717/PEERJ.10712

Johansen, K., Duan, Q., Tu, Y.-H., Searle, C., Wu, D., Phinn, S., Robson, A., & McCabe, M. F.

(2020). Mapping the condition of macadamia tree crops using multi-spectral UAV and WorldView-3 imagery. ISPRS Journal of Photogrammetry and Remote Sensing, 165, 28–

40.

Judge, R., Choi, F., & Helmuth, B. (2018). Recent Advances in Data Logging for Intertidal Ecology. Frontiers in Ecology and Evolution, 6(DEC), 1–18. https://doi.org/10.3389/fevo.2018.00213

Kiszka, J. J., Mourier, J., Gastrich, K., & Heithaus, M. R. (2016). Using unmanned aerial vehicles (UAVs) to investigate shark and ray densities in a shallow coral lagoon. Marine Ecology Progress Series, 560, 237–242. https://doi.org/10.3354/MEPS11945

Kwok, R. (2018). Ecology's remote-sensing revolution. Nature, 556(7699), 137–138.

Li, X., Tan, Y., Sun, Y., Wang, J., & Dong, Y. (2021). Microhabitat temperature variation combines with physiological variation to enhance thermal resilience of the intertidal mussel Mytilisepta virgata. Functional Ecology.

Lima, F. P., & Wethey, D. S. (2009). Robolimpets: measuring intertidal body temperatures using biomimetic loggers. Limnology and Oceanography: Methods, 7(5), 347–353. https://doi.org/10.4319/LOM.2009.7.347

Lv, M., Luan, X., Liao, C., Wang, D., Liu, D., Zhang, G., Jiang, G., & Chen, L. (2020). Human impacts on polycyclic aromatic hydrocarbon distribution in Chinese intertidal zones. Nature Sustainability 2020 3:10, 3(10), 878–884. https://doi.org/10.1038/s41893-020-0565-y

Maes, W. H., & Steppe, K. (2019). Perspectives for Remote Sensing with Unmanned Aerial Vehicles in Precision Agriculture. Trends in Plant Science, 24(2), 152–164.

https://doi.org/10.1016/J.TPLANTS.2018.11.007

Mancini, F., Dubbini, M., Gattelli, M., Stecchi, F., Fabbri, S., & Gabbianelli, G. (2013). Using unmanned aerial vehicles (UAV) for high-resolution reconstruction of topography: The structure from motion approach on coastal environments. Remote Sensing, 5(12), 6880–6898.

Marx, A., McFarlane, D., & Alzahrani, A. (2017). UAV data for multi-temporal Landsat analysis of historic reforestation: a case study in Costa Rica. International Journal of Remote Sensing, 38(8–10), 2331–2348. https://doi.org/10.1080/01431161.2017.1280637

Miner, C. M., Burnaford, J. L., Ambrose, R. F., Antrim, L., Bohlmann, H., Blanchette, C. A., Engle, J. M., Fradkin, S. C., Gaddam, R., Harley, C. D. G., Miner, B. G., Murray, S. N., Smith, J. R., Whitaker, S. G., & Raimondi, P. T. (2018). Large-scale impacts of sea star wasting disease (SSWD) on intertidal sea stars and implications for recovery. PLOS ONE, 13(3), e0192870. https://doi.org/10.1371/JOURNAL.PONE.0192870

Mozaffari, M., Saad, W., Bennis, M., Nam, Y. H., & Debbah, M. (2019). A Tutorial on UAVs for

Wireless Networks: Applications, Challenges, and Open Problems. IEEE Communications Surveys and Tutorials, 21(3), 2334–2360. https://doi.org/10.1109/COMST.2019.2902862

Murfitt, S. L., Allan, B. M., Bellgrove, A., Rattray, A., Young, M. A., & Ierodiaconou, D. (n.d.). Applications of unmanned aerial vehicles in intertidal reef monitoring OPEN. https://doi.org/10.1038/s41598-017-10818-9

Nicastro, K. R., Zardi, G. I., Teixeira, S., Neiva, J., Serrão, E. A., & Pearson, G. A. (2013). Shift happens: trailing edge contraction associated with recent warming trends threatens a distinct genetic lineage in the marine macroalga Fucus vesiculosus. https://doi.org/10.1186/17417007-11-6

NOAA's National Ocean Service. (n.d.). Retrieved August 11, 2021, from https://oceanservice.noaa.gov/

Nordlund, L. M., de la Torre-Castro, M., Erlandsson, J., Conand, C., Muthiga, N., Jiddawi, N., & Gullström, M. (2013). Intertidal Zone Management in the Western Indian Ocean: Assessing Current Status and Future Possibilities Using Expert Opinions. AMBIO 2013 43:8, 43(8), 1006–1019. https://doi.org/10.1007/S13280-013-0465-8

O'Donnell, M. J., & Denny, M. W. (2008). Hydrodynamic forces and surface topography:

Centimeter-scale spatial variation in wave forces. Limnology and Oceanography, 53(2), 579–

588. https://doi.org/10.4319/lo.2008.53.2.0579

Pádua, L., Hruška, J., Bessa, J., Adão, T., Martins, L. M., Gonçalves, J. A., Peres, E., Sousa, A. M. R., Castro, J. P., & Sousa, J. J. (2018). Multi-temporal analysis of forestry and coastal environments using UASs. Remote Sensing, 10(1), 1–21. https://doi.org/10.3390/rs10010024

Pádua, L., Vanko, J., Hruška, J., Adão, T., Sousa, J. J., Peres, E., & Morais, R. (2017). UAS, sensors, and data processing in agroforestry: a review towards practical applications. Https://Doi.Org/10.1080/01431161.2017.1297548, 38(8–10), 2349–2391. https://doi.org/10.1080/01431161.2017.1297548

Puliti, S., Ørka, H. O., Gobakken, T., & Næsset, E. (2015). Inventory of Small Forest Areas Using an Unmanned Aerial System. Remote Sensing 2015, Vol. 7, Pages 9632-9654, 7(8), 9632– 9654. https://doi.org/10.3390/RS70809632

Raffaelli, D., & Hawkins, S. (1996). Intertidal Ecology. In Intergovernmental Panel on Climate

Change (Ed.), Climate Change 2013 - The Physical Science Basis (Vol. 53, Issue 9). Springer Netherlands. https://doi.org/10.1007/978-94-009-1489-6

Raoult, V., & Gaston, T. F. (2018). Rapid biomass and size-frequency estimates of edible jellyfish populations using drones. Fisheries Research, 207, 160–164. https://doi.org/10.1016/J.FISHRES.2018.06.010

Raoult, Vincent, Colefax, A. P., Allan, B. M., Cagnazzi, D., Castelblanco-Martínez, N., Ierodiaconou, D., Johnston, D. W., Landeo-Yauri, S., Lyons, M., Pirotta, V., Schofield, G., & Butcher, P. A. (2020). Operational Protocols for the Use of Drones in Marine Animal

Research. Drones 2020, Vol. 4, Page 64, 4(4), 64. https://doi.org/10.3390/DRONES4040064

Raoult, Vincent, Tosetto, L., & Williamson, J. E. (2018). Drone-Based High-Resolution Tracking of Aquatic Vertebrates. Drones 2018, Vol. 2, Page 37, 2(4), 37. https://doi.org/10.3390/DRONES2040037

Rossiter, T., Furey, T., McCarthy, T., & Stengel, D. B. (2020). UAV-mounted hyperspectral mapping of intertidal macroalgae. Estuarine, Coastal and Shelf Science, 242, 106789. https://doi.org/10.1016/J.ECSS.2020.106789

Schneider, K. R., Van Thiel, L. E., & Helmuth, B. (2010). Interactive effects of food availability and aerial body temperature on the survival of two intertidal Mytilus species. Journal of Thermal Biology, 35(4), 161–166. https://doi.org/10.1016/J.JTHERBIO.2010.02.003

Schofield, G., Esteban, N., Katselidis, K. A., & Hays, G. C. (2019). Drones for research on sea turtles and other marine vertebrates – A review. Biological Conservation, 238, 108214. https://doi.org/10.1016/J.BIOCON.2019.108214

Seabra, R., Wethey, D. S., Santos, A. M., & Lima, F. P. (2011). Side matters: Microhabitat influence on intertidal heat stress over a large geographical scale. Journal of Experimental

Marine Biology and Ecology, 400(1–2), 200–208. https://doi.org/10.1016/j.jembe.2011.02.010

Sinclair, B. J., Marshall, K. E., Sewell, M. A., Levesque, D. L., Willett, C. S., Slotsbo, S., Dong, Y., Harley, C. D. G., Marshall, D. J., Helmuth, B. S., & Huey, R. B. (2016). Can we predict ectotherm responses to climate change using thermal performance curves and body temperatures? Ecology Letters, 19(11), 1372–1385. https://doi.org/10.1111/ELE.12686

Wang, H.-Y., Tsang, L. M., Lima, F. P., Seabra, R., Ganmanee, M., Williams, G. A., & Chan, B.

K. K. (2020). Spatial Variation in Thermal Stress Experienced by Barnacles on Rocky Shores: The Interplay Between Geographic Variation, Tidal Cycles and Microhabitat Temperatures. Frontiers in Marine Science.

Widdows, J., & Brinsley, M. (2002). Impact of biotic and abiotic processes on sediment dynamics and the consequences to the structure and functioning of the intertidal zone. Journal of Sea Research, 48(2), 143–156. https://doi.org/10.1016/S1385-1101(02)00148-X

Yao, H., Qin, R., & Chen, X. (2019). Unmanned Aerial Vehicle for Remote Sensing Applications—

A Review. Remote Sensing 2019, Vol. 11, Page 1443, 11(12), 1443. https://doi.org/10.3390/RS11121443

Zhang, J., Hu, J., Lian, J., Fan, Z., Ouyang, X., & Ye, W. (2016). Seeing the forest from drones:

Testing the potential of lightweight drones as a tool for long-term forest monitoring. Biological

Conservation, 198, 60–69. https://doi.org/10.1016/J.BIOCON.2016.03.027